DOE/ET-53088-598 IFSR #598

Electromagnetic Effect on the Toroidal Ion Temperature Gradient Mode

J.Y. KIM, W. HORTON and
J.Q. DONG
Institute for Fusion Studies
The University of Texas at Austin
Austin, Texas 78712

June 1993

Electromagnetic Effect on the Toroidal Ion Temperature Gradient Mode

J.Y. Kim, W. Horton, and J.Q. Dong
Institute for Fusion Studies
The University of Texas at Austin
Austin, Texas 78712

Abstract

A systematic study of the electromagnetic effects on the toroidal ion temperature gradient mode is presented using the local and nonlocal theories with the full kinetic terms. For the nonlocal study, a numerical code is developed to solve the electromagnetic gyrokinetic equation in the ballooning space. The electromagnetic coupling to the shear Alfvén mode is shown to give a stabilization of the toroidal temperature gradient mode at almost the same plasma pressure as that at which the kinetically modified magnetohydrodynamic (MHD) ballooning mode becomes destabilized. The transitional β-value is shown to be lower in the full kinetic description than in the fluid theory. Possible correlations of these stability results with experimental observations are discussed.

PACS Nos.: 52.25.Fp, 52.35 Kt, 52.35 Qz, 52.55 Fa.

I Introduction

The ion temperature gradient mode (η_i mode) has received considerable theoretical and experimental interests in relation to the important problem of understanding the anomalous ion thermal transport phenomena in high ion temperature plasmas. Recently, many experimental[1−5] and theoretical attempts[6−7] have been performed to test the hypothesis that the anomalous ion thermal transport is due to the η_i mode. These studies show that there are still many problems in explaining the anomalous ion thermal transport using the η_i transport model even though there exist some broad features of agreement. This situation suggests that either another instability mechanism might be responsible for the anomalous ion transport, or, that the present theoretical η_i transport models might be still incomplete. Among these two possibilities, the second is still important since many present theoretical η_i transport models are based on various approximations in its linear and nonlinear description. To obtain a clear answer, more complete analyses of the linear and nonlinear behavior of the η_i mode need to be performed through more advanced analytical methods and numerical simulations. In particular, the more exact treatments of the kinetic and toroidal effects seem to be important.

In this work, we perform a more complete analysis of the linear stability of the toroidal η_i mode in the full kinetic limit and in the electromagnetic regime. A main motivation for the present study is related with the observed χ_i behavior in the high temperature core region. Most experimental results show that the χ_i decreases in the core region with increasing temperature. This behavior is surprising since the simple mixing length estimate predicts the strong temperature dependence of the χ_i ($\propto T_i^{3/2}$ assuming $T_i \sim T_e$) so that the ion thermal conductivity should be large in the core region with the high temperature if the temperature profile is not close to the marginal state profile. Early calculations by

approximate models gave the threshold temperature gradient value η_c, which is not close to the measured η_i, and thus predicting a large χ_i in the core region in disagreement with the experiment. Here, we note that in the core region a small excess of η_i above the η_c can yield a significantly large χ_i due to the high temperature. Thus, it is important to perform more complete linear stability analysis in the core region than in the other region. The observed small χ_i in the core region suggests that the plasma must be near marginal state, that is, $\eta_i \sim \eta_c$, and we should be careful in treating various stabilizing factors which are possible in the core region.

Here, we review briefly four important stabilizing factors which may be important in the core region. The first is the temperature ratio T_i/T_e between the ion and electron, which is typically larger than one in the hot ion or supershot plasma. The large T_i/T_e is well known to give a significant stabilization on both the slab[8] and toroidal[9,10] η_i modes when the density profile is not so peaked. The second stabilizing factor is the parallel ion transit term $k_{\|} v_{\|}$, which is known to give stabilization to the toroidal η_i mode,[10–12] and can be large in the core region with small q by the dependence of $k_{\|} \propto 1/q$. The third factor is the effect of the impurity[11,13,14] and beam ions,[15,16] which can also give a significant stabilization of the η_i mode through the dilution of the main ion density. Finally, a stabilization is possible from the electromagnetic effect which occurs in the finite β plasma. When we calculate the η_c or χ_i in the core region, we should consider all of these stabilizing factors, if possible, to obtain a more exact value.

In this work, we consider in some detail the electromagnetic effect among these various stabilizing factors. In fact, there are numerous previous works[17–21] which have considered the electromagnetic effect on the toroidal η_i mode in the various limits. For example, Cheng[17] has used an approximate kinetic theory to show that the two modes of the toroidal η_i and the magnetohydrodynamic (MHD) ballooning mode coexist in the finite β toroidal plasma. Horton *et al.*[18] gave a comprehensive local kinetic analysis to study the coupling

and the transition between the electrostatic η_i mode and the MHD ballooning mode. On the other hand, Dominguez and Moore[19] and Jarmen *et al.*[20] have shown that the toroidal η_i mode tends to be stabilized by increasing β using an advanced hybrid-fluid model equations which include the kinetic effect due to the toroidal magnetic curvature drift resonance but neglect the parallel ion transit drift effect. Recently, Hong *et al.*[21] studied the effect using a more improved fluid model where the finite ion Larmor radius (FLR) and the toroidal magnetic curvature drift effects are fully considered, while the parallel ion transit drift term is considered to the first order, to show the stabilizing effect of the electromagnetic term on the toroidal η_i mode.

Compared with these previous studies, in this work we consider the electromagnetic effect of the toroidal η_i mode in the full kinetic limit which includes the resonance effects due to the toroidal magnetic curvature drift and the parallel ion transit drift, and the FLR effect. Also, unlike the previous works where more or equal emphases have been put on the stability property of the ballooning mode rather than the toroidal η_i mode, in this work we mainly concentrate on the toroidal η_i mode. We develop a numerical code to solve the electromagnetic gyrokinetic equation in the ballooning space. We also present a detailed local fluid and kinetic analysis to obtain some physical understanding of the electromagnetic effect. In this work, however, we do not consider the effects by the trapped particles and the variation of the parallel or perpendicular velocity along the field line. This our work can be considered as an extension of a recent work by Dong *et al.*[10] to include the electromagnetic effect. On the other hand, compared with the well-known code by Rewoldt *et al.*,[22] which includes all the effects mentioned above, our code may be considered as a benchmark code which concentrates on the electromagnetic effect. The relevant problems such as how the electromagnetic effect is changed by the trapped particles or how the trapped particle mode is affected by the electromagnetic effect, will be an interesting future project.

A main result of present study is that the electromagnetic effect can be important in the

actual low β plasma, in particular, in the core region. Many previous works have shown that the electromagnetic effect is stabilizing but becomes effective only when β is near $\beta_c^{\rm MHD}$, the MHD ballooning mode threshold value. Thus, for the typical discharges with $\beta \ll \beta_c^{\rm MHD}$ the effect was expected to be small. Our study, however, shows that in the full kinetic limit the toroidal η_i mode can be stabilized at the β value which is significantly lower than the value $\beta_c^{\rm MHD}$. By the same kinetic effect, the ballooning threshold value β_c itself becomes smaller than the fluid value $\beta_c^{\rm MHD}$, but this is not a so-serious problem since the real frequency of the kinetic ballooning mode is much larger than the growth rate and thus it is expected to give a weak transport effect on the ions.

In Sec. II we explain briefly our numerical method for solving the electromagnetic gyrokinetic equation in the ballooning space. We extend the integral equation method used in Refs. 9–10, to include the electromagnetic effect. A simple local fluid analysis is presented in Sec. III to obtain some physical understanding of the electromagnetic effect. In Sec. IV, we present a detailed numerical analysis of the electromagnetic effect using the local and nonlocal kinetic codes. Also, the possible correlations of the electromagnetic effect with the experimental observations are discussed. Finally, conclusion is given in Sec. V.

II Electromagnetic Integral Equation Formalism

In the low β axisymmetric toroidal system, the dynamics of the low frequency electromagnetic fluctuation is described by the quasineutrality condition

$$\int f_i \, d^3v = \int f_e \, d^3v \ , \tag{1}$$

and the parallel Ampére's law

$$-\frac{4\pi}{c} J_\parallel = \nabla_\perp^2 A_\parallel = -k_\perp^2 A_\parallel = \frac{4\pi e}{c} \left(\int v_\parallel f_e d^3v - \int v_\parallel f_i \, d^3v \right) \ , \tag{2}$$

with

$$f_j(\mathbf{v},\theta) = -\frac{q_j\, F_{Mj}}{T_j}\,\phi(\theta) + h_j(v_\perp, v_\|, \theta) J_0(\delta_j)\ , \qquad j = i, e\ , \tag{3}$$

and the nonadiabatic response $h_j(v_\perp, v_\|, \theta)$ which is determined from the gyrokinetic equation in the ballooning space

$$\left(i\,\frac{v_\|}{Rq}\,\frac{\partial}{\partial\theta} + \omega - \omega_{Dj}\right) h_j = \frac{q_j\, F_{Mj}}{T_j}\,(\omega - \omega_{*j}^T)\, J_0(\delta_j)\left[\phi(\theta) - \frac{v_\|}{c}\, A_\|(\theta)\right]\ , \tag{4}$$

where

$$\omega_{Dj} = \widehat{\omega}_{Dj}\left(\frac{v_\perp^2}{2} + v_\|^2\right)/2v_{tj}^2\ ,$$

$$\omega_{*j}^T = \omega_{*j}\left[1 + \eta_j\left(\frac{v^2}{2v_{tj}^2} - \frac{3}{2}\right)\right]\ ,$$

$$\widehat{\omega}_{Dj} = 2\epsilon_n \omega_{*j}\left[\cos\theta + \sin\theta(s\theta - \alpha\sin\theta)\right]\ ,$$

$$k_\perp^2 = k_y^2\left[1 + (s\theta - \alpha\sin\theta)\right]^2\ ,$$

with $\delta_j = \frac{k_\perp v_\perp}{\omega_{cj}}$, $\omega_{*j} = -\frac{c\,k_\theta\, T_j}{q_j\, B\, L_{nj}}$, $\eta_j = \frac{d\ln n}{d\ln T_j}$, $\alpha = -\frac{2Rq^2}{B^2}\frac{dp}{dr}$, $\omega_{cj} = \frac{eB}{m_j c}$, $v_{tj} = \left(\frac{T_j}{m_j}\right)^{1/2}$, $L_n = -\left(\frac{d\ln n}{dr}\right)^{-1}$, $\varepsilon_n = \frac{L_n}{R}$, $s = \frac{r}{q}\frac{dq}{dr}$, $F_{Mj} = (2\pi\, v_{tj}^2)^{-3/2}\exp(-v^2/2v_{tj}^2)$, and J_0 is the Bessel function of zeroth order.

In Eq. (4), we note that the well-known ballooning representation

$$\widetilde{f} = \sum_{m=-\infty}^{\infty} e^{im\theta}\int_{-\infty}^{\infty} e^{-im\theta'} e^{in(\xi - q\theta') - i\omega t} f(\theta')\, d\theta'\ , \tag{5}$$

where ξ and θ are the toroidal and extended poloidal angles, respectively, has been used and the usual $s-\alpha$ equilibrium model has been adapted.

As mentioned in the introduction, we do not consider the trapped particles effect in this work. Equations (4) can then be easily integrated with the boundary condition $h(\theta) = 0$ as $|\theta| \to \infty$ to give the following solution for h

$$v_\| > 0\ ,\ h_j = -i\frac{q_j\, F_{Mj}}{T_j}\int_{-\infty}^{\theta} d\theta'\,\frac{qR}{|v_\||}\, e^{i(\sigma_j - \sigma_j')}(\omega - \omega_{*j}^T)\, J_0(\delta_j')\left[\phi(\theta') - \frac{|v_\||}{c}\, A_\|(\theta')\right], \tag{6}$$

$$v_\| < 0\ ,\ h_j = -i\frac{q_j\, F_{Mj}}{T_j}\int_{\theta}^{\infty} d\theta'\,\frac{qR}{|v_\||}\, e^{-i(\sigma_j - \sigma_j')}(\omega - \omega_{*j}^T)\, J_0(\delta_j')\left[\phi(\theta') + \frac{|v_\||}{c}\, A_\|(\theta')\right], \tag{7}$$

with

$$\sigma_j(\theta) = \int_{\theta_0}^{\theta} d\theta' \, \frac{qR}{|v_{\|}|} [\omega - \omega_{Dj}(\theta')] \; , \tag{8}$$

$\sigma'_j = \sigma_j(\theta')$ and $\delta'_j = \delta_j(\theta')$.

Now, substituting Eqs. (6) and (7) into Eqs. (1) and (2), we obtain the following two integral equations

$$\left(1 + \frac{T_i}{T_e}\right) \phi(\theta) = \sum_j \int_{-\infty}^{+\infty} d\theta' \left[K_j^0(\theta,\theta')\phi(\theta') - K_j^1(\theta,\theta')\widehat{A}_{\|}(\theta')\right] \; , \tag{9}$$

$$\frac{c^2 T_i}{4\pi \, N \, e^2 \, v_{ti}^2} \, k_\perp^2 \, \widehat{A}_{\|}(\theta) = \sum_j \int_{-\infty}^{+\infty} d\theta' \left[K_j^1(\theta,\theta')\phi(\theta') - K_j^2(\theta,\theta')\widehat{A}_{\|}(\theta')\right] \; , \tag{10}$$

where

$$K_j^m(\theta,\theta') = \int_0^\infty 2\pi \, v_\perp \, dv_\perp \int_0^\infty dv_{\|} \left[\frac{v_{\|}}{v_{ti}} \operatorname{sgn}(\theta - \theta')\right]^m G_j(v_\perp, v_{\|}, \theta, \theta') \; , \tag{11}$$

with

$$G_j(v_\perp, v_{\|}, \theta, \theta') = -i \, \frac{T_i}{T_j} \, \frac{qR}{v_{\|}} \, e^{i(\sigma_j - \sigma'_j)\operatorname{sgn}(\theta-\theta')} (\omega - \omega_{*j}^T) J_0(\delta_j) \, J_0(\delta'_j) \, F_{Mj} \; ,$$

and $\widehat{A}_{\|}(\theta) = \frac{v_{ti}}{c} A_{\|}(\theta)$.

A major simplification in the integration of Eq. (11) is possible if we neglect the $v_{\|}$ modulation along the unperturbed particle orbit due to the equilibrium magnetic field. This assumption is also concurrent with the above neglect of the trapped particles effect. Then, for the ions, the $v_\perp$ integration in Eq. (11) can be performed analytically yielding

$$K_i^m(\theta,\theta') = -i \int_0^\infty dv_{\|} \, v_{\|}^{m-1} \, g(v_{\|}, \theta, \theta') \; , \tag{12}$$

where

$$g(v_{\|}, \theta, \theta') = \frac{qR}{(2\pi)^{1/2} \, v_{ti}} \exp\left[-v_{\|}^2/2 - i \operatorname{sgn}(\theta - \theta')(\sigma_0 - \sigma'_0) \, v_{\|} + i\omega \, qR|\theta - \theta'|/v_{ti} \, v_{\|}\right]$$

$$\times \left[\omega - \omega_{*i}\left(1 + \eta_i \left(\frac{v_{\|}^2}{2} - \frac{d}{d\lambda} - \frac{3}{2}\right)\right)\right] \frac{1}{\lambda} I_0 \left(\frac{\sqrt{b_i b'_i}}{\lambda}\right) e^{-(b_i + b'_i)/2\lambda} \; , \tag{13}$$

with

$$\lambda = 1 + i(\sigma_0 - \sigma_0')\,\mathrm{sgn}\,(\theta - \theta')/v_{\|}\ ,$$

$$\sigma_0 = \frac{1}{2}\int_{\theta_0}^{\theta} d\theta'\,\frac{qR}{v_{ti}}\,\widehat{\omega}_{Di}(\theta')\ ,$$

$$b_i = k_\perp^2(\theta)\rho_i^2\ .$$

On the other hand, for the electron, we use the ordering $\omega \sim \omega_{Di} \sim \omega_{De} \ll |k_{\|}v_{te}|$. Then, the velocity integration can be done easily, yielding to the first order,

$$K_e^0 \simeq 0\ , \tag{14}$$

$$K_e^1 \simeq \frac{q\,RT_i}{2v_{ti}\,T_e}(\omega - \omega_{*e})\,\mathrm{sgn}(\theta - \theta')\ , \tag{15}$$

$$K_e^2 \simeq i\frac{q^2\,R^2\,T_i}{2v_{ti}^2\,T_e}\left[\omega(\omega - \omega_{*e})|\theta - \theta'| - \mathrm{sgn}\,(\theta - \theta')(\sigma_1 - \sigma_1')(\omega - \omega_{*pe})\right]\ , \tag{16}$$

with $\sigma_1 = \int_{\theta_0}^{\theta} d\theta'\widehat{\omega}_{De}(\theta')/2$ and $\omega_{*pe} = \omega_{*e}(1 + \eta_e)$.

In this work we solve the integral equations (9) and (10), with the kernels given in Eq. (12) and Eqs. (14)–(16). As in the electrostatic case, the kernels in Eq. (11) have the symmetry property of $K^m(\theta, \theta') = (-1)^m K^m(\theta', \theta)$ and have the logarithmic singularity at $\theta = \theta'$ which can be treated easily by standard numerical method. This electromagnetic integral equation code is a straightforward extension of that used in Refs. 9–10 to include the electromagnetic effect. However, compared with the electrostatic code which can be used only for the study of the η_i mode, this electromagnetic code can be used also for the study of the kinetically-modified ideal ballooning mode.

While the nonlocal integral equation code is most desirable to obtain the exact eigenvalue of the toroidal η_i mode, it is still useful to consider the simpler local kinetic limit. Taking the local approximations of $k_{\|} = -\frac{i}{Rq}\frac{\partial}{\partial\theta}$, $\widehat{\omega}_D = \widehat{\omega}_D(\theta = 0) = 2\varepsilon_n\omega_*$, and $k_\perp = k_y$, we can easily obtain the following local kinetic equations from Eqs. (1)–(2), in the dimensionless form,

$$\omega(1 + \tau - P_0)\phi = (\tau(\omega - \omega_{*e}) - k_{\|}P_1)\psi\ , \tag{17}$$

$$\frac{2k_{\|}^2\,k_{\perp}^2}{\beta_i}\,\psi = \omega\left[k_{\|}\,P_1 - \tau(\omega-\omega_{*e})\right]\phi - \left[k_{\|}^2\,P_2 - \tau(\omega(\omega-\omega_{*e}) - \omega_{De}(\omega-\omega_{*pe}))\right]\psi\ , \quad (18)$$

where

$$P_m = \int (v_{\|})^m\,\frac{\omega-\omega_{*i}\left(1+\eta_i\left(\frac{v^2}{2}-\frac{3}{2}\right)\right)}{\omega-\epsilon_n\omega_{*i}\left(\frac{v_{\perp}^2}{2}+v_{\|}^2\right)-k_{\|}\,v_{\|}}\,J_0^2(k_{\perp}\,v_{\perp})e^{-\frac{v^2}{2}}v_{\perp}\,dv_{\perp}\,\frac{dv_{\|}}{\sqrt{2\pi}}\ , \quad (19)$$

with $\tau = T_i/T_e$, $\beta_i = 8\pi\,N\,T_i/B^2$, $\omega_{*e} = k_y$, $\omega_{*i} = -k_y$, $\omega_{*pe} = \omega_{*e}(1+\eta_e)$, and $\psi = \frac{\omega\,v_{ti}}{ck_{\|}}\,A_{\|}$. Here, we note that the ordering of $\omega/k_{\|}\,v_{te}$, $\omega_{De}/k_{\|}\,v_{te} \ll 1$ has been used to take the first order terms only in the electron response. On the other hand, we have normalized the wavenumbers $k_{\perp}$ and $k_{\|}$ to $\rho_i = v_{ti}/\omega_{ci}$ and L_n, respectively, and the frequencies ω and ω_* to v_{ti}/L_n. Our local electromagnetic code is developed to solve Eqs. (17) and (18).

III Local Fluid Analysis

Before we present the numerical results from the local and nonlocal kinetic codes described in Sec. II, here, we first consider the simpler local fluid limit of $|\omega_D/\omega| \ll 1$, $|k_{\|}\,v_e/\omega| \ll 1$ and $k_{\perp}^2 \ll 1$ to obtain some physical understanding of the electromagnetic effect. Taking the fluid limit, Eq. (19) gives

$$P_0 \simeq 1 - \frac{\omega_{*i}}{\omega} + \left(\frac{\omega_{Di}}{\omega} - k_{\perp}^2 + \frac{k_{\|}^2}{\omega^2}\right)\left(1-\frac{\omega_{*pi}}{\omega}\right)\ ,$$

$$P_1 \simeq \frac{k_{\|}}{\omega}\left(1-\frac{\omega_{*pi}}{\omega}\right)\ , \qquad P_2 \simeq 1 - \frac{\omega_{*pi}}{\omega}\ ,$$

with $\omega_{*pi} = \omega_{*i}(1+\eta_i)$ and $\omega_{Di} = 2\varepsilon_n\omega_{*i}$, and thus Eqs. (17) and (18) reduce to, respectively,

$$\left[\tau\left(1-\frac{\omega_{*e}}{\omega}\right) - \frac{k_{\|}^2}{\omega^2}\left(1-\frac{\omega_{*pi}}{\omega}\right)\right](\phi-\psi) + \left(k_{\perp}^2 - \frac{\omega_{Di}}{\omega}\right)\left(1-\frac{\omega_{*pi}}{\omega}\right)\phi = 0\ , \quad (20)$$

$$\omega(\omega-\omega_{*pi})k_{\perp}^2\,\phi = \frac{2k_{\|}^2\,k_{\perp}^2}{\beta_i}\psi + \omega_{Di}(\omega-\omega_{*pi})\phi + \tau\omega_{De}(\omega-\omega_{*pe})\psi\ . \quad (21)$$

We note that Eqs. (20) and (21) are the well-known continuity and vorticity equations, in the incompressible MHD fluid limit. Equations (20)–(21) describe the coupling of the electrostatic drift wave and the electromagnetic shear Alfvén wave.

In the electrostatic limit of $\beta_i \to 0$, Eq. (21) gives

$$\psi = \beta_i \frac{\omega(\omega - \omega_{*pi})k_\perp^2 - \omega_{Di}(\omega - \omega_{*pi})}{2k_\parallel^2 k_\perp^2 - \beta_i \omega_{Di}(\omega - \omega_{*pe})}\phi \ll \phi \ ,$$

and Eq. (20) reduces to

$$\tau\left(1 - \frac{\omega_{*e}}{\omega}\right) - \frac{k_\parallel^2}{\omega^2}\left(1 - \frac{\omega_{*pi}}{\omega}\right) = -\left(k_\perp^2 - \frac{\omega_{Di}}{\omega}\right)\left(1 - \frac{\omega_{*pi}}{\omega}\right) \ , \tag{22}$$

which is the well-known dispersion relation of the electrostatic η_i mode equation in the local fluid limit. In Eq. (22), we note that the terms $k_\parallel^2 \omega_{*pi}$ and $\omega_{Di}\omega_{*pi}$ represent the driving forces of the slab and the toroidal η_i modes, respectively.

On the other hand, in the electromagnetic shear Alfvén limit where $\omega \simeq \omega_{*pi}$, Eq. (20) gives $\phi \simeq \psi$, and thus Eq. (21) becomes

$$\omega(\omega - \omega_{*pi})k_\perp^2 = \frac{2k_\parallel^2 k_\perp^2}{\beta_i} - \omega_{Di}(\omega_{*pi} - \omega_{*pe}) \ , \tag{23}$$

which is the well-known dispersion relation of the ideal ballooning mode equation in the local fluid limit. From Eq. (23) it is easy to see that the threshold value of β_i for the ideal ballooning instability is given by

$$\beta_{ic} = \frac{2k_\parallel^2 k_\perp^2}{\omega_{Di}(\omega_{*pi} - \omega_{*pe}) - (\omega_{*pi}k_\perp/2)^2} \ , \tag{24}$$

with the marginal real frequency of $\omega_r \simeq \omega_{*pi}/2$. Note that for the long wavelength modes with $k_\perp^2 \ll 1$ the β_{ic} reduces to $\beta_{ic} \simeq k_\parallel^2/\varepsilon_n\,[1 + \eta_i + (1+\eta_e)T_e/T_i] \sim \varepsilon_n/q^2$ with $k_\parallel \sim 1/Rq$.

Now, let us consider how the coupling with the electromagnetic shear Alfvén wave stabilizes the electrostatic toroidal η_i mode. Expressing the ψ in terms of ϕ from Eq. (21) and substituting it to Eq. (20), we obtain the following dispersion relation

$$\tau + \frac{\omega_{*i}}{\omega} - \frac{k_\parallel^2}{\omega^2}\left(1 - \frac{\omega_{*pi}}{\omega}\right) = -\left(k_\perp^2 - \frac{\omega_{Di}}{\omega}\right)\left(1 - \frac{\omega_{*pi}}{\omega}\right)\left[1 - \frac{\tau\omega(\omega - \omega_{*e}) - k_\parallel^2\left(1 - \frac{\omega_{*pi}}{\omega}\right)}{\frac{2k_\parallel^2 k_\perp^2}{\beta_i} - \omega_{Di}(\omega - \omega_{*pe})}\right] \ . \tag{25}$$

Comparing Eq. (25) with Eq. (22), we can see that the last term in the right-hand side represents the electromagnetic effect. We note that the electromagnetic effect has changed the coefficient of the destabilizing force term $\omega_{Di}\omega_{*pi}$ for the toroidal η_i mode from 1 to

$$1 - \frac{\tau\omega(\omega - \omega_{*e}) - k_{\|}^2\left(1 - \frac{\omega_{*pi}}{\omega}\right)}{\frac{2k_{\|}^2 k_{\perp}^2}{\beta_i} - \omega_{Di}(\omega - \omega_{*pe})} . \tag{26}$$

Noting $\omega \sim \omega_{Di} \ll \omega_{*pi}$ for the toroidal η_i mode, Eq. (26) says that the coefficient of the destabilizing force changes its sign at about

$$\beta_i \simeq \beta_{it} = \frac{2k_{\|}^2 k_{\perp}^2}{\omega_{Di}\left(\omega_{*i} - \omega_{*pe}\right) + \frac{k_{\|}^2 \omega_{*pi}}{\omega_{Di}}} , \tag{27}$$

so that the toroidal η_i mode is completely stabilized by the electromagnetic effect at about $\beta_i \sim \beta_{it}$.

The critical value β_{it} is almost independent of the wavenumber k_y when $k_x^2 \propto k_y^2$ and $k_{\|}^2 < \omega_{Di}^2$, and this means that the electromagnetic effect will weakly depend on the wavenumber k_y. The β_{it} is also inversely proportional to the η_i, so that the growth rate of the toroidal η_i mode is expected to increase more slowly with the increasing η_i, compared with the electrostatic case. Also, we note that $\beta_{it} \propto k_{\|}^2$ which means the smaller $k_{\|}$ will give more stabilization for a fixed plasma β_i, which is opposite to the electrostatic case of $\beta_i \to 0$ where the larger $k_{\|}$ gives more stabilization. This change of the $k_{\|}$ dependence of the growth rate suggests that in the small, but, finite β_i regime the most unstable mode occurs when the mode has an optimum, finite value of $k_{\|}$. We will present more detailed analyses of these dependences of the electromagnetic effect on the various parameters, in Sec. IV using the kinetic theory. Finally, we note from Eqs. (24) and (27) that the β_{it} has a similar form as the β_{ic}. The two critical values of the toroidal η_i mode and the ballooning mode have similar scalings in $k_{\|}$ and k_y. This means that the stabilization of the toroidal η_i mode is closely related with the generation of the electromagnetic ballooning instability. In fact, Eq. (25) shows that the excitation of the electromagnetic shear Alfvén wave weakens the driving force

of the electrostatic toroidal η_i mode.

IV Local and Nonlocal Kinetic Analyses

In the previous section, we have considered the electromagnetic effect in the local fluid limit to obtain some physical understanding. Here, we present a more detailed and exact numerical analysis of the effect using the local and nonlocal kinetic codes, based on Eqs. (17)–(18) and Eqs. (9)–(10), respectively. In particular, emphasis is put on how much the electromagnetic effect is changed by the kinetic effects.

A. Local kinetic analysis

We first analyze the electromagnetic effect using the local kinetic code. Compared with the nonlocal gyrokinetic code, the local kinetic code is much simpler and covers well the kinetic effects so that it is useful in studying various parameter dependence of the η_i mode stability.

In Fig. 1, we first show the growth rate and the real frequency as a function of β_i, when $k_y \rho_i = 0.5$, $\eta_i = 2.5$, $\eta_e = 2$, $\varepsilon_n = 0.2$, $\tau = 1$, and $k_{||} = 0.1$. Comparisons are given between the local kinetic (LK) and the local fluid (LF) cases. We first observe that in both cases the toroidal η_i mode is stabilized at the β_i value which is near the ballooning threshold value β_{ic}. As discussed in Sec. III, this means that the stabilization of the electrostatic toroidal η_i mode is closely related with the excitation of the shear Alfvén ballooning mode, even though the two modes have completely different frequency range, as shown in Fig. 1(b). Approximately, the ballooning mode has the real frequency of $\omega_r \sim \omega_{*pi}$, while the η_i mode has $\omega_r \sim \omega_{Di}$, near the threshold value of β_i in the kinetic regime.

Figure 1 also shows clearly that with the kinetic effect, the overall growth rates of the η_i mode are substantially reduced from the fluid value. An important feature of Fig. 1 is that the critical β_i values for the stabilization of the toroidal η_i mode is significantly reduced from the fluid results. The threshold value β_c for the ballooning instability is also

observed to decrease with the kinetic effect. As shown by Hong *et al.*,[21] this decrease of β_c comes mainly from the effect of the toroidal ∇B-curvature drift resonance. The stronger stabilization of the toroidal η_i mode in the full kinetic limit also comes mainly from this toroidal resonance effect. For the electromagnetic ballooning mode, the toroidal resonance gives the dissipation effect similar to the resistivity, and thus plays the role of reducing the bending force of the magnetic field line, contributing to the destabilization. On the other hand, for the electrostatic toroidal η_i mode the resonance contributes just to the Landau damping of the mode, giving the stabilization. The significant decrease of the effective β_i value for the stabilization of the toroidal η_i mode by the kinetic effects implies that the electromagnetic effect can be a more important stabilizing factor in the relatively low β plasma. In fact, as will be shown in Sec. IV.C, the stability analysis of the toroidal η_i mode for the two Tokamak Fusion Test Reactor (TFTR) supershot discharges[6] indicates that in the intermediate core region with the relatively small β_i value the electromagnetic effect can give a significant stabilization. Here, we note that the destabilization of the ideal ballooning instability at the smaller β_i value by the kinetic resonance dissipation effect is not a so-serious problem, because as shown in Fig. 1(b), the kinetic ballooning mode has the real frequency which is much larger than the growth rate and thus it is expected to give a relatively weak transport effect on the ions.

While the electromagnetic effect is dominantly determined by the parameter β_i, it can also be significantly changed by the other parameters at a given β_i value. In particular, as can be seen from Eq. (27), the electromagnetic effect is closely related to the parameter $k_{||}$. To study the effect of $k_{||}$, here we assume that $k_{||}$ is an arbitrary constant parameter even though it is actually an operator. More exact treatment of the $k_{||}$ effect will be given in the next section using the nonlocal gyrokinetic code. In Fig. 2 we show the dependence of the electromagnetic effect on $k_{||}$ for various β_i regimes with the other parameters — the same as in Fig. 1. We first observe that the stabilizing effect of the electromagnetic term at a given

β_i increases significantly as $k_{||}$ decreases. Figure 2 also shows clearly that the stabilization of the η_i mode occurs almost simultaneously with the destabilization of the ballooning mode, indicating again the close relation between the two events. As discussed in Sec. II, these features of the η_i mode stabilization and the ballooning mode destabilization occurring in the small $k_{||}$ region can be explained as such that the decreasing $k_{||}$ makes the electromagnetic shear Alfvén wave more active and thus increases the coupling between the η_i mode and the shear Alfvén wave. The excited shear Alfvén wave develops to the ballooning mode as β_{ic} becomes smaller than β_i with the decreasing $k_{||}$. Finally, in Fig. 2 we note that in the large $k_{||}$ region where the electromagnetic effect is small, the growth rate decreases strongly with the increasing $k_{||}$. As is well known,[10–12] this stabilization by the large $k_{||}$ comes from the stabilizing effect of the parallel ion transit term. Now, by these two different stabilizing factors in the small and large limits of $k_{||}$, the mode becomes most unstable when it has a proper intermediate $k_{||}$ value.

The local stability analysis in Sec. III suggests from Eq. (27) that the stabilization degree of the toroidal η_i mode by the electromagnetic effect will weakly depend on the wavenumber k_y. In Fig. 3, the growth rate of the toroidal η_i mode is shown as a function of $k_y\rho_i$ for various values of β_i with the other parameters same as Fig. 1. We first observe that the maximum growth rate occurs around $k_y\rho_i \sim 0.5$ and this location of the peak growth rate in wavenumber space does not change so much when β_i increases. The stabilization by the electromagnetic effect occurs almost uniformly in the wavenumber region above the peak growth rate wavenumber of $k_y\rho_i \geq 0.5$. On the other hand, in the long wavelength region of $k_y\rho_i \leq 0.5$ the stabilization due to the finite β_i becomes ineffective as the $k_y\rho_i$ decreases. This behaviour in the long wavelength region occurs since in this region the stabilizing effect due to the parallel ion transit drift term $k_{||}\, v_i$ becomes relatively stronger than the stabilizing effect due to the electromagnetic coupling. Note that the ratio $k_{||}\, v_i/\omega_D$ between the two drift terms $k_{||}\, v_i$ and $\omega_D(\propto k_y)$ increases as the k_y decreases, and that the strong stabilization

of the toroidal η_i mode in the long wavelength region comes from this increase of the $k_{\|} v_i$ effect.

The equation (27) from the local fluid analysis also suggests that the dependence of the growth rate on η_i will become weaker in the electromagnetic regime. In Fig. 4 we show how the dependence of the growth rate on η_i changes with the β_i value. It is found that the stabilization by the electromagnetic effect occurs more strongly in the large η_i region so that the positive slope of the growth rate versus η_i decreases significantly with the increasing β_i. This change of the scaling of the growth rate on η_i due to the electromagnetic effect is a particular feature of the toroidal η_i mode and suggests that if the anomalous ion thermal transport occurs mainly due to the toroidal η_i mode, the ion thermal conductivity χ_i should weakly depend on the η_i in the finite β plasma. Finally, from the curve at $\beta_i = 0.006$ in Fig. 4 we note that in similar with the toroidal η_i mode the growth rate of the kinetic ballooning mode also does not increase monotonically with η_i, but takes a maximum value at a proper η_i.

B. Non-local gyrokinetic analysis

In the previous subsection, we have used the simple local kinetic theory to investigate various aspects of the electromagnetic effect. While this local theory appears to be reliable and useful for the study of the kinetic or electromagnetic effects on the toroidal η_i mode stability in a wide range of parameters, it is still incomplete in several aspects. In particular, the local theory can not treat exactly the effect of the parameters such as q and s, even though we can obtain some estimate through the parameter $k_{\|}$.

To complement this local kinetic analysis, here we present some nonlocal stability analyses using the gyrokinetic code introduced in Sec. II. While this nonlocal gyrokinetic code is more accurate and thus should be used to estimate more exactly the growth rate in the actual system, in this work we limit our concern to the study of the dependence of the

electromagnetic effect on the parameters such as q and s, which were not covered by the local kinetic analyses in the previous section. Noting the strong dependence of the electromagnetic effect on $k_{||}$ and the close relation between the operator $k_{||}$ and the parameters q and s, it is expected that the electromagnetic effect will depend significantly on the parameters q and s. The present electromagnetic, integral equation analysis also provides a more complete estimate of the dependence of the toroidal η_i mode stability on q and s parameters than the previous electrostatic[10] or differential equation[21] analyses, and can be important in relation to the interpretation of a recent current ramp perturbative experiment.[3]

In Fig. 5 we first show a typical structure of the eigenfunction of the toroidal η_i mode in the ballooning space, obtained from the nonlocal gyrokinetic equation code for the parameters set of $\eta_i = 2.5$, $\eta_e = 2$, $k_y \rho_i = 0.5$, $\varepsilon_n = 0.2$, $\tau = 1$, $s = 0.6$, $q = 1.5$, and $\beta_i = 0.004$. We observe that the two fluctuation variables ϕ and $\widehat{A}_{||}$ ($\equiv \frac{v_{ti}}{c} A_{||}$) have even and odd parities in the ballooning θ space, respectively, and that $|\widehat{A}_{||}/\phi| \ll 1$ for the toroidal η_i mode in the low β plasma.

In Fig. 6 we show the growth rate as a function of q and s at various β_i values, when $\eta_i = 2.5$, $\eta_e = 2$, $k_y \rho_i = 0.5$, $\varepsilon_n = 0.2$, and $\tau = 1$. First, in Fig. 6(a) we note that when $s = 0.6$ the figure is almost symmetric with Fig. 2. This relation is easily understood if we note that the $k_{||} = -i \frac{1}{Rq} \frac{\partial}{\partial \theta}$ is almost inversely proportional to q, so that the large q corresponds to the small $k_{||}$, vice versa. From this relation between $k_{||}$ and q, we can see that the stabilization at small q region is mainly due to the parallel ion transit drift, while the stabilization at large q region comes from the electromagnetic effect. Comparing the two cases of $s = 0.6$ and 2 in Fig. 6(a), we find that the q effect at a given β_i is significantly changed with the shear s. Figure 6(a) shows that the growth rate curve $\gamma(q)$ at a given β_i has shifted substantially to the larger q region when s is increased from 0.6 to 2. This result means that the stabilizing effect by the parallel ion transit term in the small q region increases significantly with the increasing shear, while the stabilizing effect by the electromagnetic

term in the large q region decreases with the increasing shear. This feature appears more clearly in Fig. 6(b), which shows the growth rate as a function of s for given q and β_i values and the other parameters, as in Fig. 6(a). This result of the shear effect may be understood easily from the relation between s and $k_{||}$. It is obvious that as s increases the mode width of the eigenfunction becomes narrow through the term $k_\perp^2 = k_y^2(1 + s^2\theta^2)$ within the finite Larmor radius term J_0 in Eq. (4), which mainly determines the mode width in the ballooning θ space. This decrease of the mode width produces the increase of $k_{||}$ since the average $k_{||}$ will increase almost inversely proportional to the mode width $\Delta\theta$. Now, as shown in Fig. 2, the increase of the average $k_{||}$ in turn means the increase of the parallel ion transit term and also the decrease of the electromagnetic effect. Thus, the shear effects shown in Fig. 6 can be explained well through the relation between s and $k_{||}$. In summary, Fig. 6 shows that the electromagnetic effect at a given finite β_i becomes effective as q increases and s decreases. In the typical tokamak system, the parameters q and s increase almost simultaneously with the minor radius. Thus, the average $k_{||}$ will be almost constant over the minor radius, and the electromagnetic effect is expected to come mainly through the term β_i which strongly decreases with the minor radius.

C. Correlations with experimental trends

There are some experimental trends in the large, high temperature plasma tokamaks which seem to suggest that the electromagnetic effect gives actually an important stabilization. First, in Fig. 7 we show the maximum growth rate as a function of the minor radius, calculated for the TFTR 44669A supershot discharge[6] using the electrostatic and electromagnetic codes. In the electromagnetic case, the nonlocal results are also compared with the local results maximized over $k_{||}$. Note that the nonlocal code gives more stabilization than the local code. Figure 7 shows clearly that the maximum growth rates are significantly reduced by the electromagnetic effect in the intermediate core region, even though near the edge re-

gion, the effect is negligible. The TFTR 44669 discharge data shows that in the intermediate region of $0.2 < r/a < 0.5$ where the electromagnetic stabilization is significant the β_i value ranges about from 0.002 to 0.006 with $\beta_e < \beta_i$, and thus the plasma is in the relatively low β regime. It might be worthwhile to note here that the strong stabilization, shown in the deep core region of $r < 0.2$m in Fig. 7, comes mainly from the large T_i/T_e effect which is an another stabilizing factor.

Secondly, in Fig. 8, we show the ion thermal conductivity χ_i as a function of the minor radius, calculated using the simple mixing length formula with the $\gamma_{\max}$ and $k_{\max}$ which are obtained from the nonlocal electrostatic and electromagnetic codes for the two supershot discharges of TFTR 44669A and TFTR 51025. Also shown are the experimental results. We can see that the χ_i's are in much better agreement with the experimental results in the intermediate core region when the electromagnetic effect is included, even though there is still a large discrepancy between the theoretical and experimental values in the outer half region. These results suggest the importance of the electromagnetic effect in the bulk region of the relatively low β plasma.

On the other hand, comparing a recent hot ion H-mode experiment by Taroni *et al.* in Joint European Torus (JET)[4] with the TFTR 44669A supershot experiment,[2] we find that TFTR has much larger χ_i value (about 4-5 times on the average) than JET, while the two experiments have almost the same magnitude and profile in T_i, T_e, n_e. A main difference between the two experiments is that the JET plasma has the β_i value which is about three times larger than that of the TFTR because the toroidal magnetic field of TFTR is about 1.7 larger than the JET field. This simple comparison suggests, even though there can be other possibilities such as the q profile and geometry effects, that the smaller value of the χ_i in JET may be related to the larger electromagnetic effect from the three times higher β_i.

Also, a recent experiment[5] of the L to H transition in DIII-D by Burrell *et al.* shows the significant decrease of the χ_i as well as χ_e, after the L to H transition. This H-mode

confinement improvement is found to occur in the both regions of the plasma edge and the bulk of the plasma. While the confinement improvement in the edge region is well recognized due to the transport barrier related to the poloidal shear flow, there seems to be no proper model to explain the confinement improvement in the bulk region. There are no appreciable changes in the profiles of $T_{i,e}$ and q, while a significant change occurs in the density profile with an increase in the density itself, during the L to H transition. Thus, the confinement improvement in the bulk region should be closely related to these changes in the density and its profile. In terms of the electrostatic η_i mode the improved confinement is then difficult to understand since the flattening of the density profile or the increase of the density is not the stabilizing factor of the mode (the electrostatic dispersion relation is independent of density). On the other hand, including the electromagnetic effect an explanation is possible in terms of the η_i mode that the decrease of χ_i may be relevant to the enhanced electromagnetic effect due to the increased density, even though it still does not explain well the significant decrease of the χ_e.

Finally, a recent experiment by Hirayama *et al.*[23] in JT-60 shows that when the density only is increased by about two times there is a significant decrease of the χ_i in the core region, while no appreciable change occurs in the χ_e.

All three experiments suggest that the electromagnetic effect is playing an important role in determining the plasma thermal confinement, in particular, in the core region.

V Conclusion

In this work, we have analyzed the electromagnetic effect on the toroidal η_i mode in the full kinetic limit. Using the local and nonlocal eigenmode analyses, we have shown that the electromagnetic effect gives the stabilization on the toroidal η_i mode through the coupling with the finite shear Alfvén mode, and the threshold β value for the stabilization of η_i mode is almost equal to that for the kinetically modified MHD ballooning mode to be generated. In

particular, we have shown that the electromagnetic effect gives a more significant stabilization in the low β plasma when the full kinetic terms are included, suggesting that the effect can be an important stabilizing factor, in addition to the other stabilizing factors such as the large T_i/T_e, the beam and impurity effects, to explain the decrease of the ion thermal conductivity χ_i in the core region. In this work, we have not considered the effect of the trapped particle dynamics which was shown to make the electromagnetic effect weaker in a recent work[24] within the context of a simple model. We will consider the trapped electron effect later using the more complete code even though in the core region with the small fraction of the trapped particles the effect is expected not to be significant.

Acknowledgments

We would like to S.D. Scott, M.C. Zarnstorff, and other TFTR experimental team for useful discussions and for providing the discharge data. This work is supported by the U.S. Department of Energy contract #DE-FG05-80ET-53088.

References

1. S.D. Scott, P.H. Diamond, R.J. Fonck, R.B. Howell, K.P. Jahnig, G. Schilling, E.J. Synakowski, M.C. Zarnstorff, C.E. Bush, E. Fredrickson, K.W. Hill, A.C. Janos, D.K. Mansfield, D.K. Owens, H. Park, G. Pautasso, A.T. Ramsey, J. Schivell, G.D. Tait, W.M. Tang, and G. Taylor, Phys. Rev. Lett. **64**, 531 (1990).

2. S.D. Scott, V. Arunasalam, C. W. Barnes, M.G. Bell, M. Bitter, R. Boivin, N.L. Bretz, R. Bundy, C.E. Bush, A. Cavallo, T.K. Chu, S.A. Cohen, P. Colestock, S.L. Davis, D.L. Dimock, H.F. Dylla, P.C. Efthimion, A.B. Erhrardt, R.J. Fonck, E. Fredrickson, H.P. Furth, R.J. Goldston, G. Greene, B. Grek, L.R. Grisham, G. Hammett, R.J. Hawryluk, H.W. Hendel, K.W. Hill, E. Hinnov, D.J. Hoffman, J. Hosea, R.B. Howell, H. Hsuan, R.A. Hilse, K.P. Jaehnig, A.C. Janos, D. Jassby, F. Jobes, D.W. Johnson, L.C. Johnson, R. Kaita, C. Kiera-Phillips, S.J. Kilpatrick, P.H. LaMarche, B. LeBlane, R. Little, D.M. Manos, D.K. Mansfield, E. Mazzucato, M.P. MaCarthy, D.C. McCune, K. McGuire, D.H. McNeill, D.M. Meade, S.S. Medley, D.R. Mikkelsen, R. Motley, D. Mueller, J.A. Murphy, Y. Nagayama, R. Nazakian, D.K. Owens, H. Park, A.T. Ramsey, M.H. Redi, A.L. Roquemore, P.H. Rutherford, G. Schilling, J. Schivell, G.L. Schmidt, J. Stevens, B.C. Stratton, W. Stodiek, E.J. Synakowski, W.M. Tang, G. Taylor, J.R. Timberlake, H.H. Towner, M. Ulrickson, S. von Goeler, R. Wieland, M. Williams, J.R. Wilson, K.-L. Wong, S. Yoshikawa, K.M. Young, M.C. Zarnstorff, and S.J. Zweben, Phys. Fluids B **2**, 1300 (1990).

3. M.C. Zarnstorff, C.W. Barnes, P.C. Efthimion, G.W. Hammett, W. Horton, R.A. Hulse, D.K. Mansfield, E.S. Marmar, K.M. McGuire, G. Rewoldt, E.J. Synakowski, W.M. Tang, J.L. Terry, X.Q. Xu, M.G. Bell, M. Bitter, N.L. Bretz, R. Bundy, C.E. Bush, P.H. Diamond, R.J. Fonck, E. Fredrickson, H.P. Furth, R.J. Goldstone, B. Grek,

R.J. Hawryluk, K.W. Hill, H. Hsuan, D.W. Johnson D.C. McCune, D.M. Meade, D. Mueller, D.K. Owens, H.K. Park, A.T. Ramsey, M.N. Rosenbluth, J. Schivell, G.L. Schmidt, S.D. Scott, G. Taylor, and R.M. Wieland, in *Plasma Physics and Controlled Nuclear Fusion Research, 1990*, Proceedings of the 12th International Conference, Washington (IAEA, Vienna, 1991), vol. I, p. 109.

4. A. Taroni, F. Tibone, B. Balet, D. Boucher, J.P. Chistiansen, J.D. Cordey, G.C. Corrigan, D.F. Duchs, R. Giannella, A. Gondhalekar, N. Gottardi, G.M.D. Hogeweij, L. Lauro-Taroni. K. Lawson. M. Mattioli, D. Muir, J. O'rourke, D. Pasini, P.H. Rebut, C. Sack, G. Sips, E. Springmann, T.E. Springer, P. Stubberfield, K. Thomson, M.L. Watkins, and H. Weisen, in *Plasma Physics and Controlled Nuclear Fusion Research, 1990*, Proceedings of the 12th International Conference, Washington (IAEA, Vienna, 1991), vol. I, p. 93.

5. K.H. Burrell, R.J. Groebner, T.S. Kurki-Suonio, T.N. Carlstrom, R.R. Dominguez, P. Gohil, R.A. Jong, H. Matsumoto, J.M. Lohr, T.W. Petrie, G.D. Porter, G.T. Sager, H.E. St. John, D.P. Schissel, S.M. Wolfe, and the DIII-D Research Group, in *Plasma Physics and Controlled Nuclear Fusion Research, 1990*, Proceedings of the 12th International Conference, Washington (IAEA, Vienna, 1991), vol. 1, p. 123.

6. W. Horton, D. Lindberg, J.-Y. Kim, J.Q. Dong, G.W. Hammett, S.D. Scott, M.C. Zarnstorff, and S. Hamaguchi, Phys. Fluids B **4**, 953 (1992).

7. M. Kotschenreuther, H.L. Berk, R. Denton, S. Hamaguchi, W. Horton, C.-B. Kim, M. Lebrun, P. Lyster, S. Mahajan, W.H. Miner, P.J. Morrison, D. Ross, T. Tajima, J.B. Talyor, P.M. Valanju, H.V. Wong, S.Y. Xiao, and Y.-Z. Zhang, in *Plasma Physics and Controlled Nuclear Fusion Research*, 1990, Proceedings of the 12th International Conference, Washington (IAEA, Vienna, 1991), Vol. II. p. 361.

8. T.S. Hahm and W.M. Tang, Phys. Fluids B **1**, 1185 (1989).

9. F. Romanelli, Phys. Fluids B **1**, 1018 (1989).

10. J.Q. Dong, W. Horton, and J.Y. Kim, Phys. Fluids B **4**, 1867 (1992).

11. R.R. Dominguez and M.N. Rosenbluth, Nucl. Fusion **29**, 844 (1989).

12. J.Y. Kim and W. Horton, Phys. Fluids B **3**, 1167 (1991).

13. P. Terry, W. Anderson, and W. Horton, Nucl. Fusion **22**, 487 (1982).

14. R. Peccagnella, F. Romanelli, and S. Briguglio, Nucl. Fusion **30**, 545 (1990).

15. M. Liljestrom, Nucl. Fusion **30**, 2611 (1990).

16. W. Horton, J.Y. Kim, J.Q. Dong, and M. Kotschenreuther, IFS News Lett. **9**, 2 (1993).

17. C.Z. Cheng, Nucl. Fusion **22**, 773 (1982).

18. W. Horton, J.E. Sedlak, D.I. Choi, and B.G. Hong, Phys. Fluids **28**, 3050 (1985).

19. R.R. Dominguez, and R.W. Moore, Nucl. Fusion **26**, 85 (1986).

20. A. Jarmen, P. Anderson, and J. Weiland, Nucl. Fusion **27**, 941 (1987).

21. B.G. Hong, W. Horton, and D.I. Choi, Plasma Phys. Controlled Fusion **31**, 1291 (1989); B.G. Hong, W. Horton, and D.I. Choi, Phys. Fluids B **1**, 1589 (1989).

22. G. Rewoldt, W.M. Tang, and M.S. Chance, Phys. Fluids **25**, 480 (1982).

23. T. Hirayama, H. Shirai, M. Yagi, K. Shimizu, Y. Koide, M. Kikuchi, and M. Azumi, Nucl. Fusion **32**, 89 (1992).

24. J. Weiland and A. Hirose, Nucl. Fusion **32**, 151 (1992).

Figure Captions

1. The normalized growth rate (a) and the real frequency (b) of the toroidal η_i mode (solid line) and the ideal ballooning mode (dotted line) as a function of β_i in the local kinetic (LK) and local fluid (LF) limits when $\eta_i = 2.5$, $\eta_e = 2$, $k_y\rho_i = 0.5$, $k_{\|} = 0.1$, $\varepsilon_n = 0.2$, and $\tau = 1$.

2. The normalized growth rate of the toroidal η_i mode (solid line) and the ideal ballooning mode (dotted line) as a function of $k_{\|}$ for various β_i values with other parameters same as Fig. 1.

3. The normalized growth rate of the toroidal η_i mode as a function of $k_y\rho_i$ for various β_i values with other parameters same as Fig. 1.

4. The normalized growth rate of the toroidal η_i mode as a function of η_i for various β_i values with other parameters same as Fig. 1.

5. The mode structure of an electromagnetic toroidal η_i mode in the ballooning space when $\eta_i = 2.5$, $\eta_e = 2$, $k_y\,\rho_i = 0.5$, $\varepsilon_n = 0.2$, $\tau = 1$, $s = 0.6$, $q = 1.5$ and $\beta_i = 0.004$.

6. The normalized growth rate of the toroidal η_i mode for various β_i values; (a) as a function of q for two s values, (b) as a function of s for two q values, when $\eta_i = 2.5$, $\eta_e = 2$, $k_y\,\rho_i = 0.5$, $\varepsilon_n = 0.2$, and $\tau = 1$.

7. The maximum growth rate of the toroidal η_i mode as a function of the minor radius for the TFTR 44669A supershot discharge.

8. The ion thermal conductivity χ_i, calculated using the mixing length formula, as a function of the minor radius for the two TFTR supershot discharges of (a) 44669A (b) 51025.

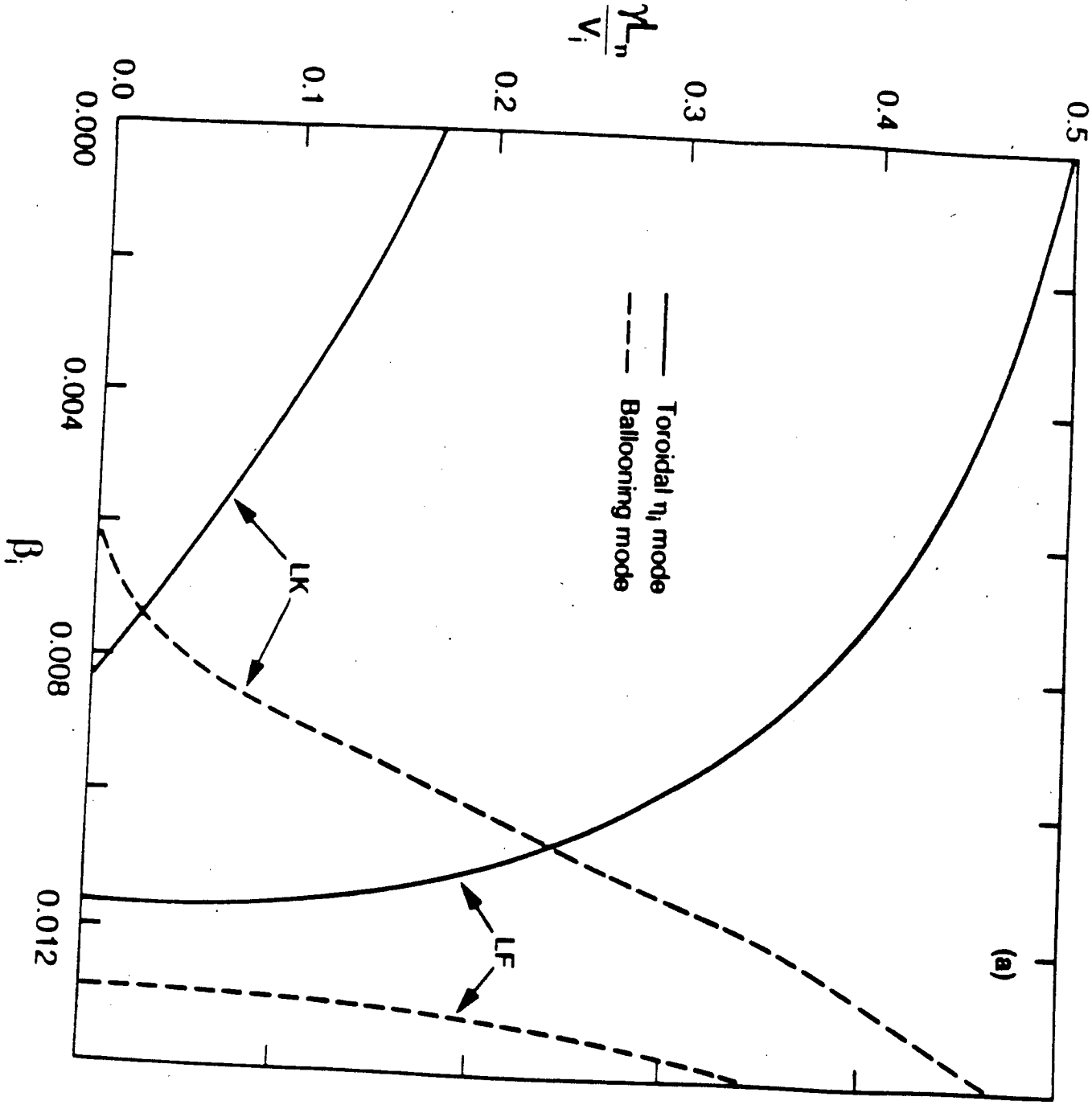
(a)
0.5
0.4
0.3
0.2
0.1
0.0
$\frac{\gamma L_n}{v_i}$
Toroidal η_i mode
Ballooning mode
LK
LF
0.000
0.004
0.008
0.012
β_i

Fig. 1(a)

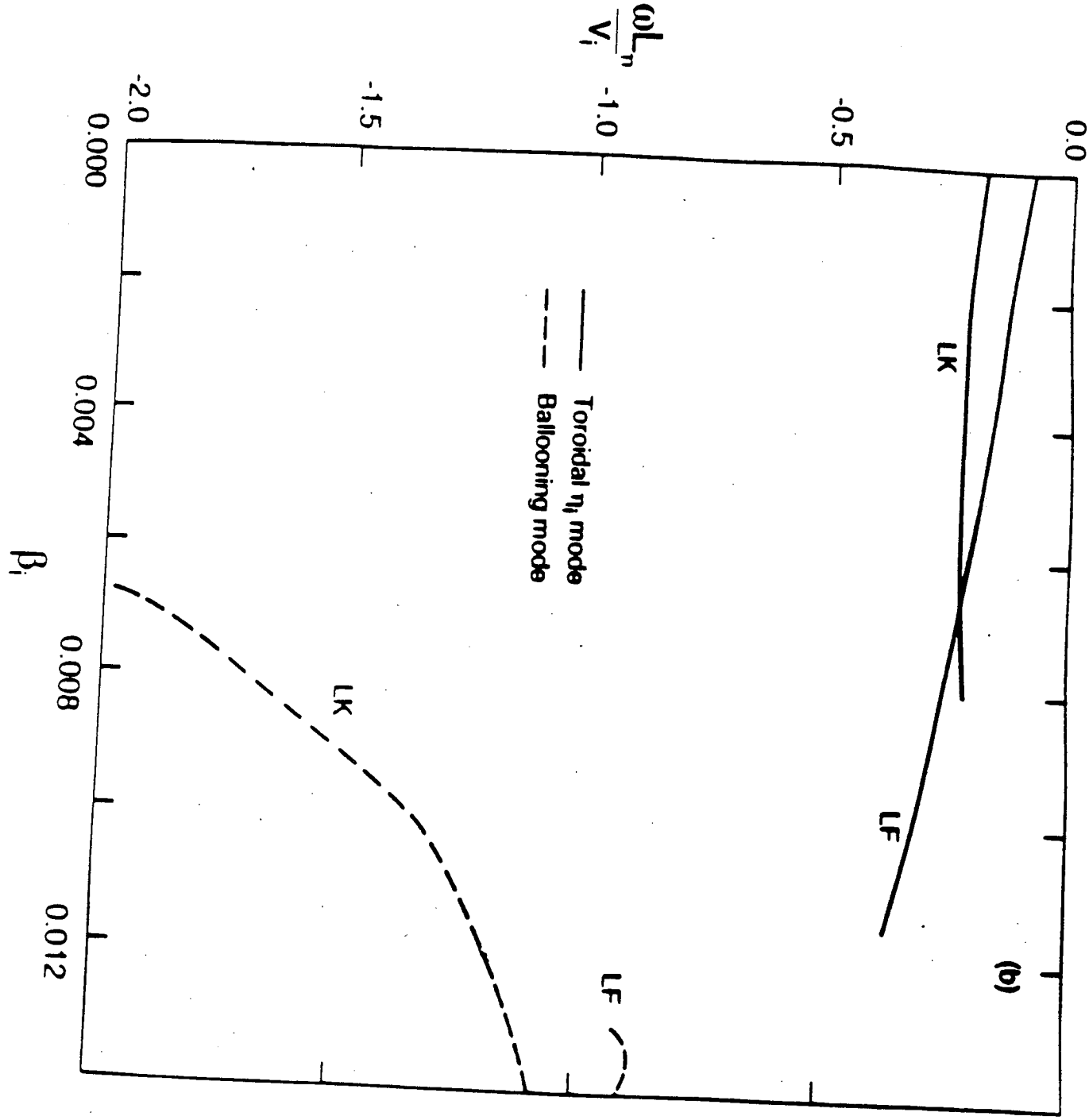
0.0
-0.5
-1.0
-1.5
-2.0
$\frac{\omega L_n}{V_i}$
0.000
0.004
0.008
0.012
β_i
LK
LF
LK
LF
Toroidal η_i mode
Ballooning mode
(b)

Fig. 1(b)

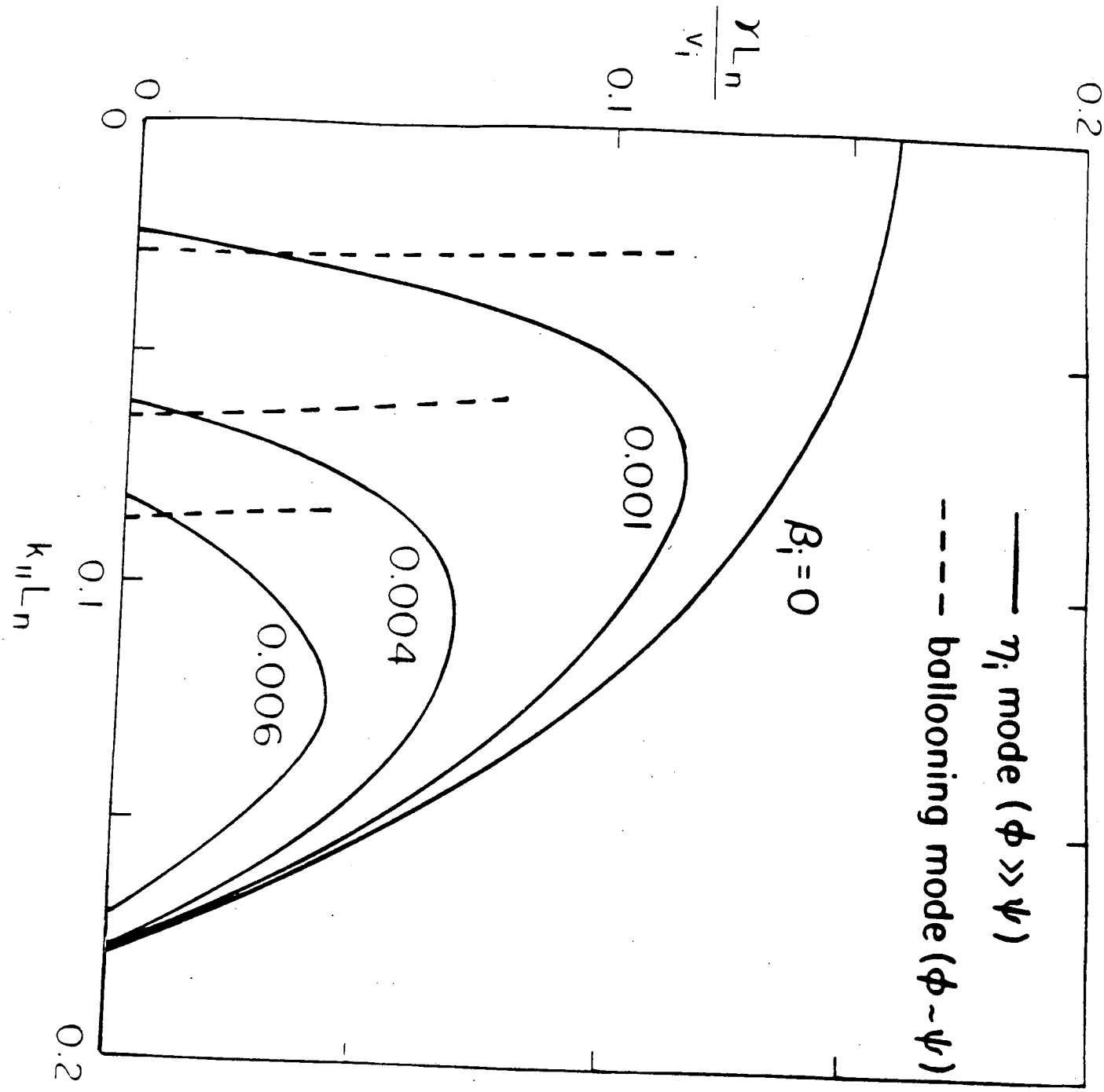
0.2
$\frac{\gamma L_n}{v_i}$
0.1
0
0.001
0.004
0.006
$\beta_i = 0$
η_i mode ($\phi \gg \psi$)
balooning mode ($\phi \sim \psi$)
0
0.1
0.2
$k_{\parallel} L_n$

Fig. 2

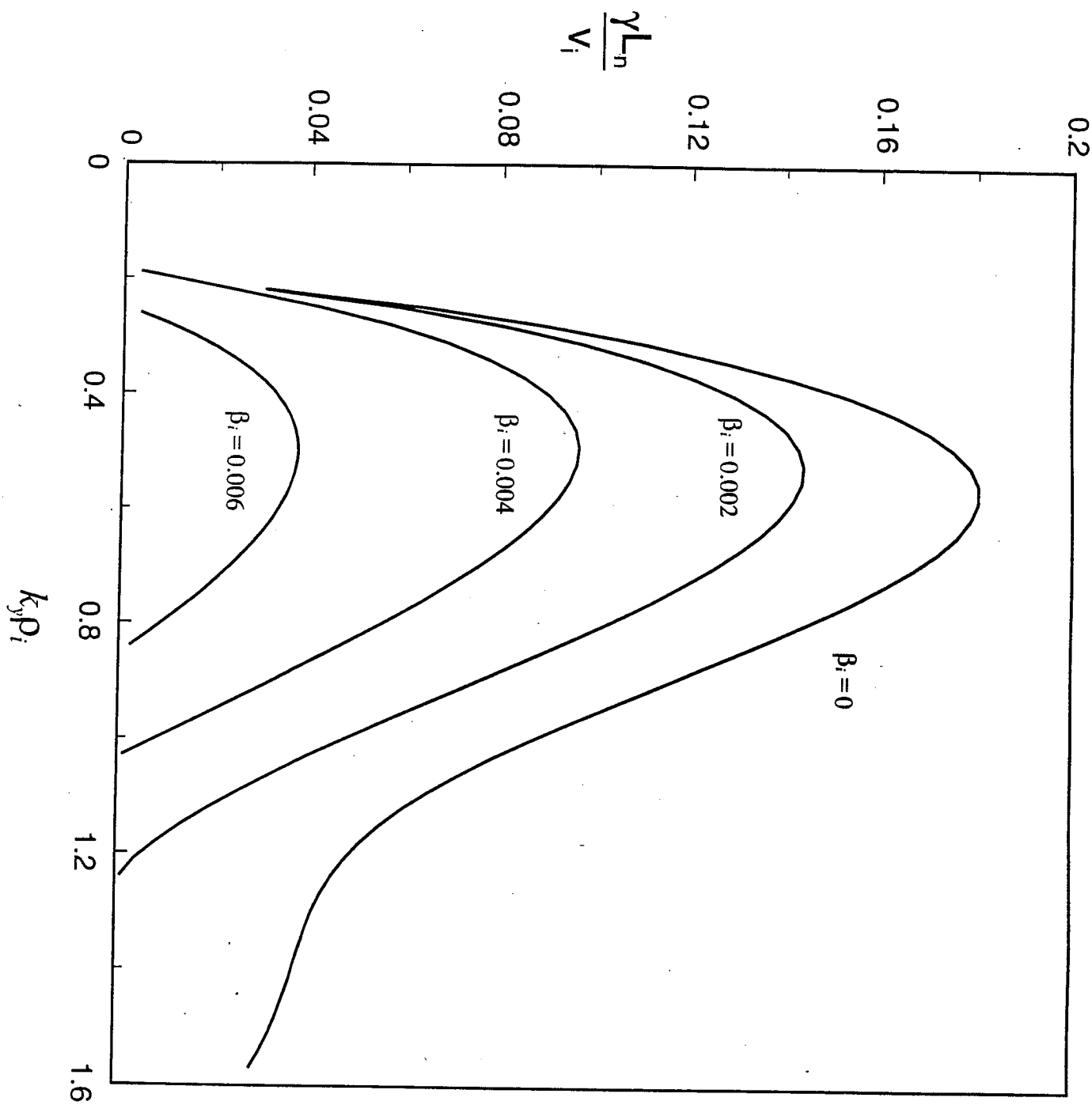
0.2
0.16
0.12
0.08
0.04
0
$\frac{\gamma L_n}{v_i}$
0
0.4
0.8
1.2
1.6
$k_y \rho_i$
$\beta_i = 0$
$\beta_i = 0.002$
$\beta_i = 0.004$
$\beta_i = 0.006$

Fig. 3

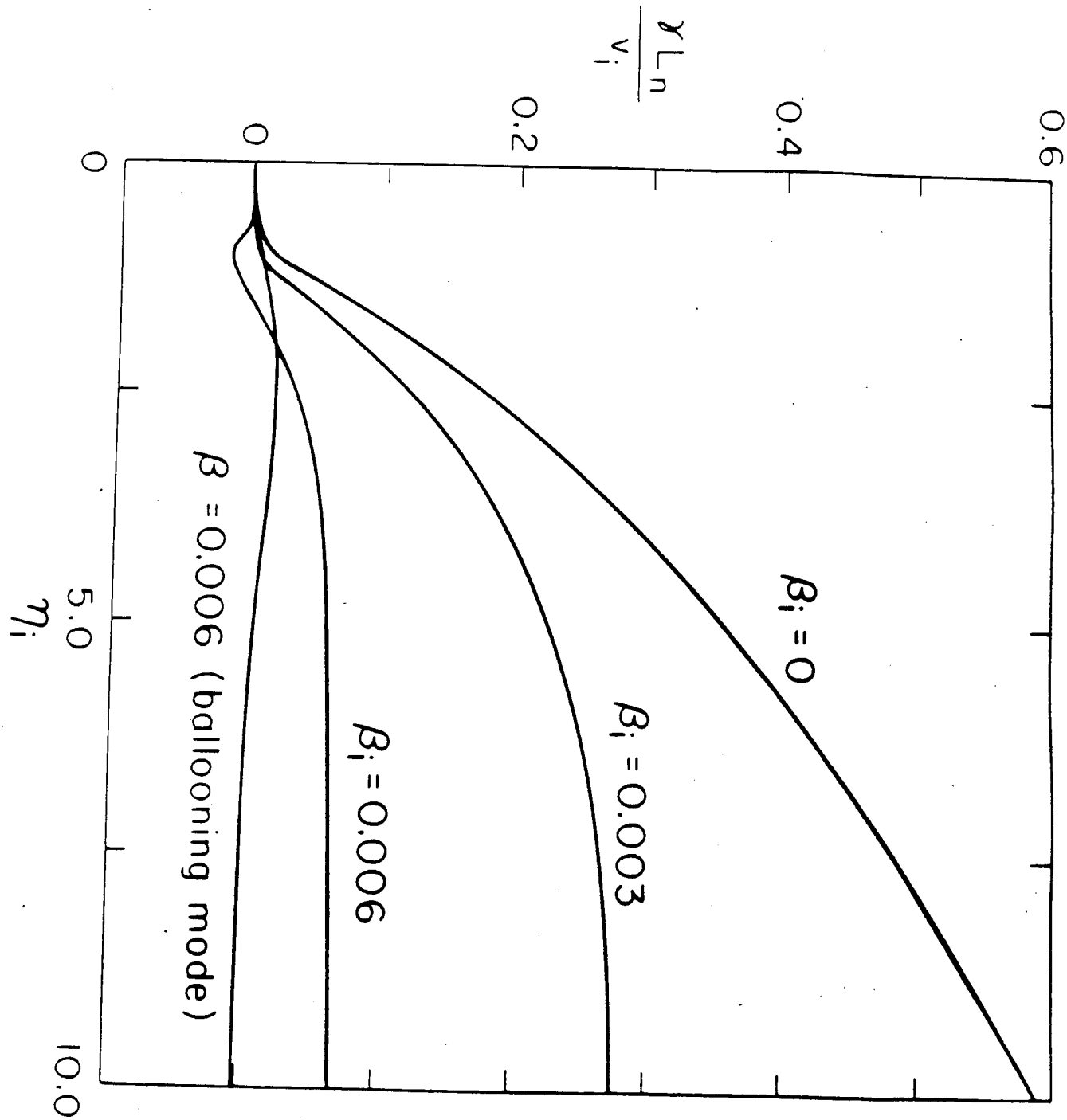
0.6
0.4
0.2
0
$\frac{\gamma L_n}{v_i}$
$\beta_i = 0$
$\beta_i = 0.003$
$\beta_i = 0.006$
$\beta = 0.006$ (ballooning mode)
0
5.0
10.0
η_i

Fig. 4

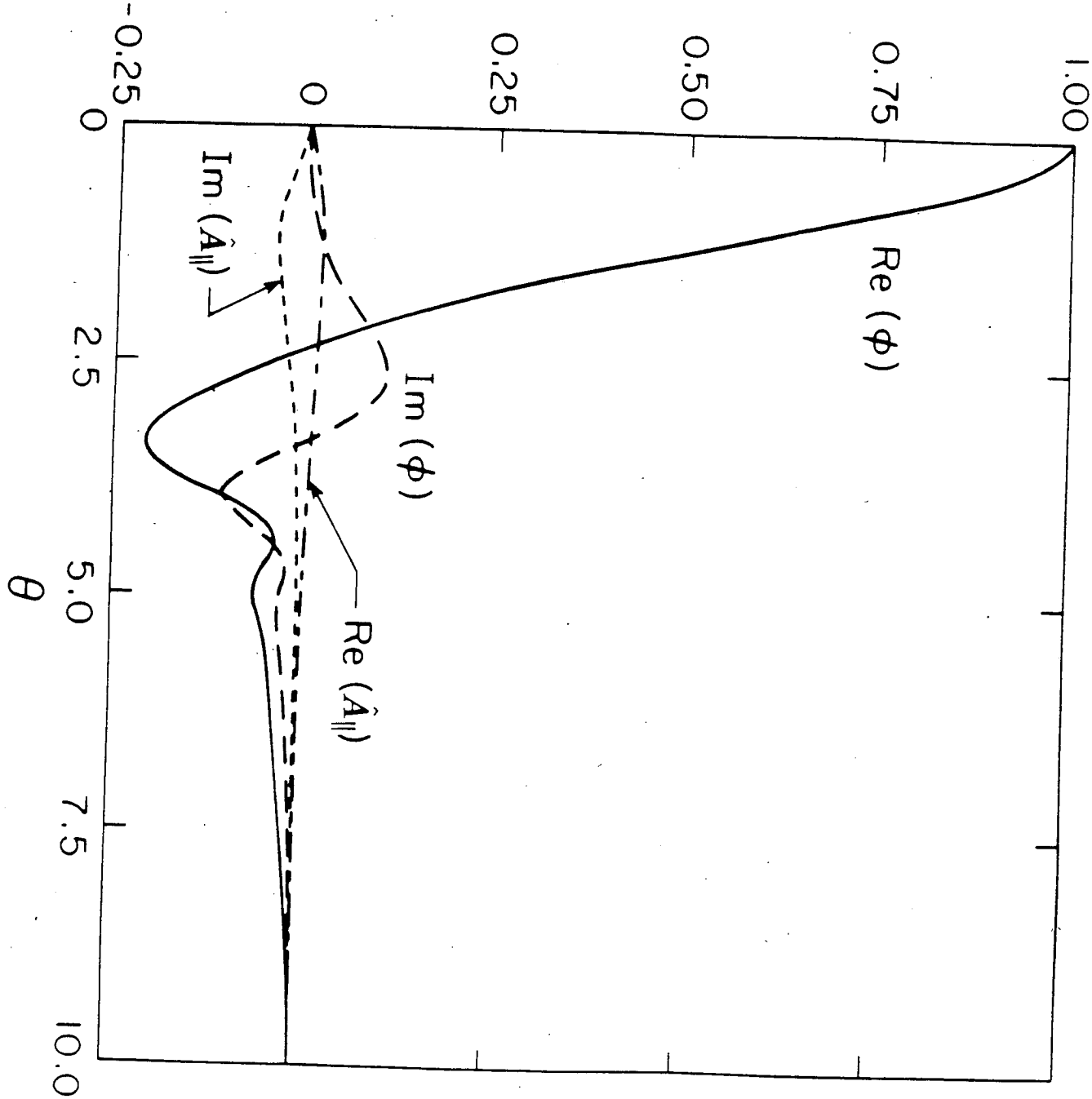
1.00
0.75
0.50
0.25
0
-0.25
Re (ϕ)
Im (ϕ)
Re ($\hat{A}_{\parallel}$)
Im ($\hat{A}_{\parallel}$)
0
2.5
5.0
7.5
10.0
θ

Fig. 5

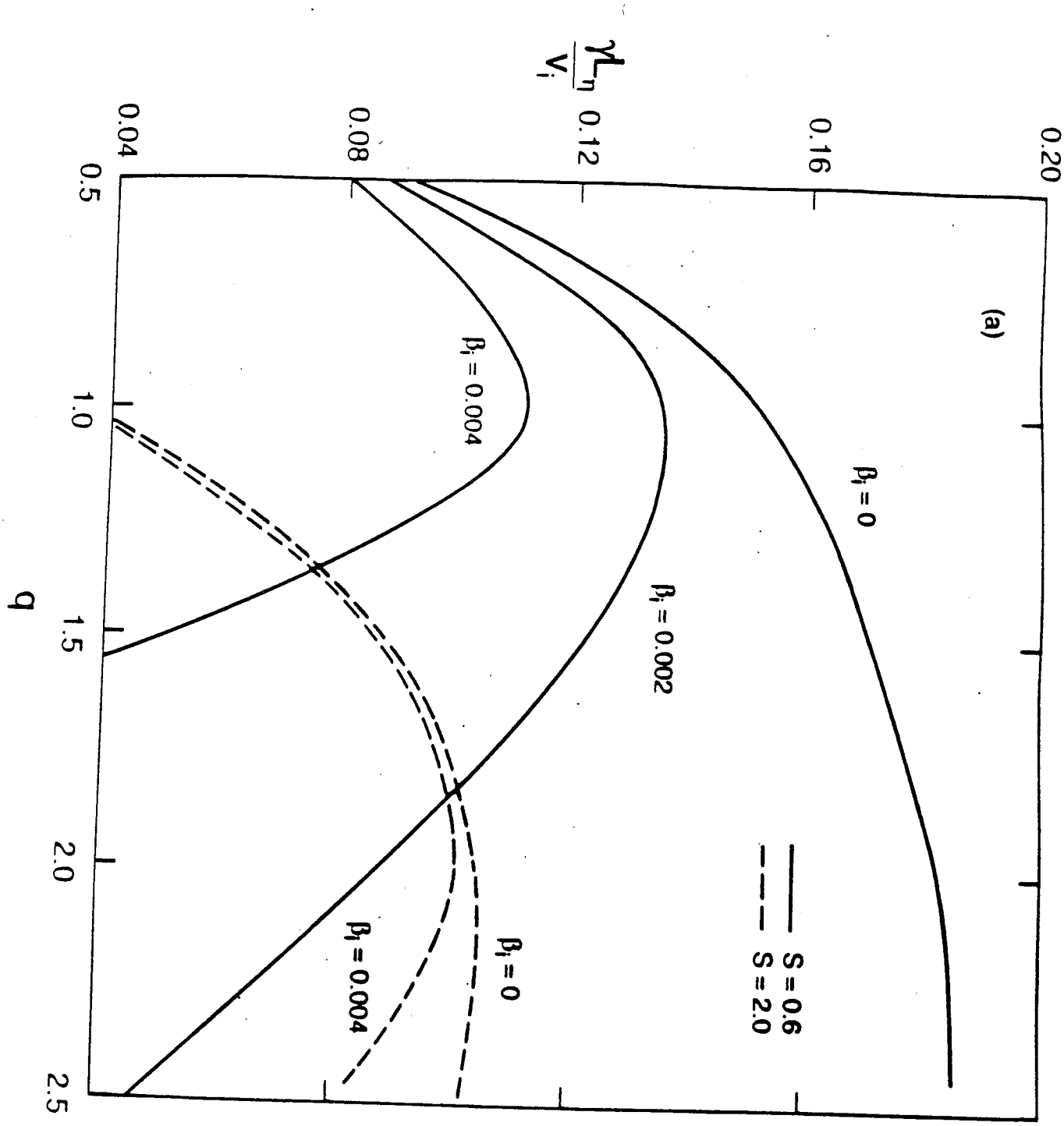
(a)
0.20
0.16
0.12
0.08
0.04
$\frac{\gamma L_\eta}{V_i}$
0.5
1.0
1.5
2.0
2.5
q
$\beta_i = 0$
$\beta_i = 0.002$
$\beta_i = 0.004$
$\beta_i = 0$
$\beta_i = 0.004$
S = 0.6
S = 2.0

Fig. 6(a)

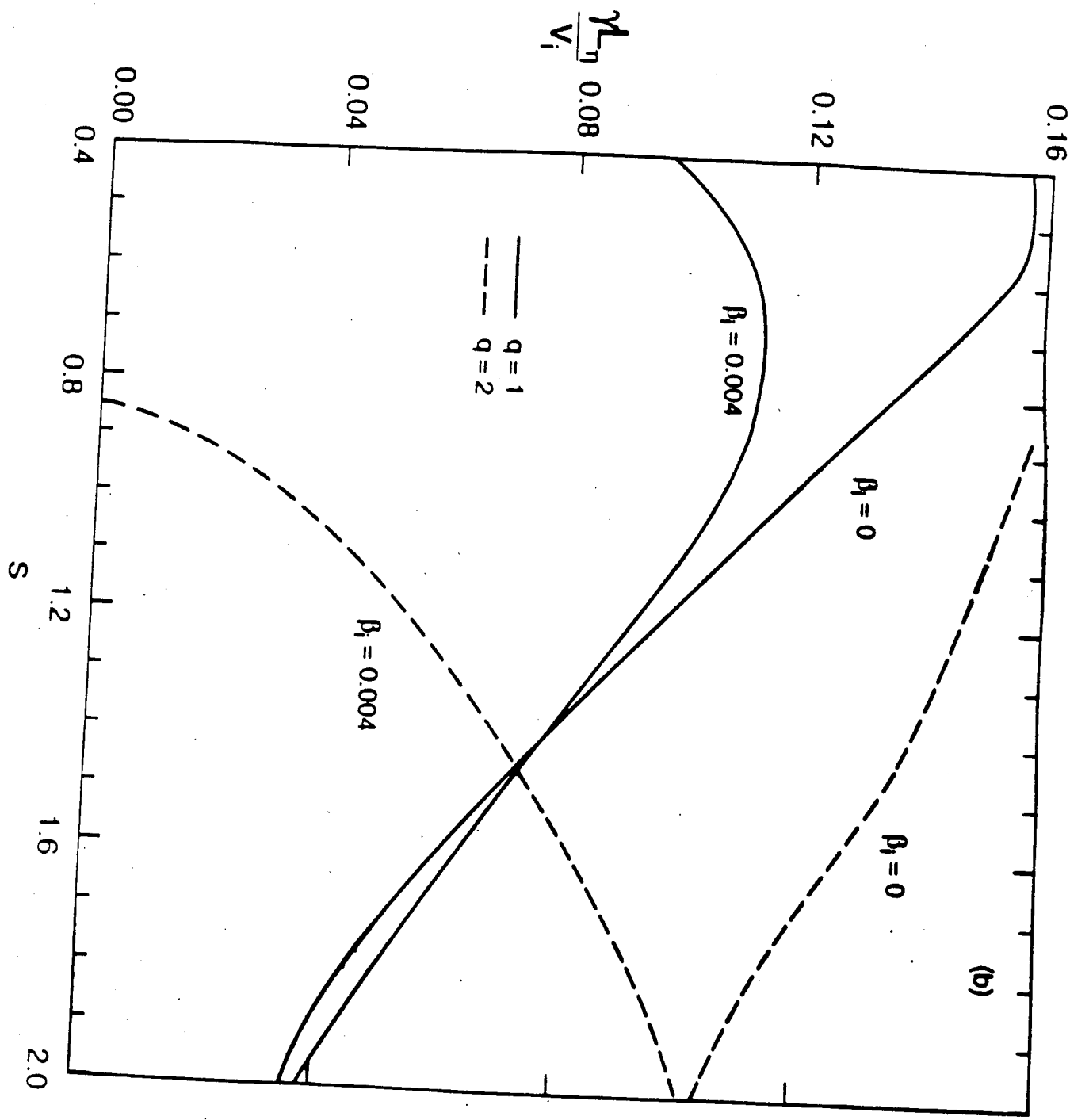
0.16
0.12
0.08
0.04
0.00
$\frac{\gamma L_\eta}{V_i}$
0.4
0.8
1.2
1.6
2.0
S
(b)
$\beta_i = 0$
$\beta_i = 0$
$\beta_i = 0.004$
$\beta_i = 0.004$
q = 1
q = 2

Fig. 6(b)

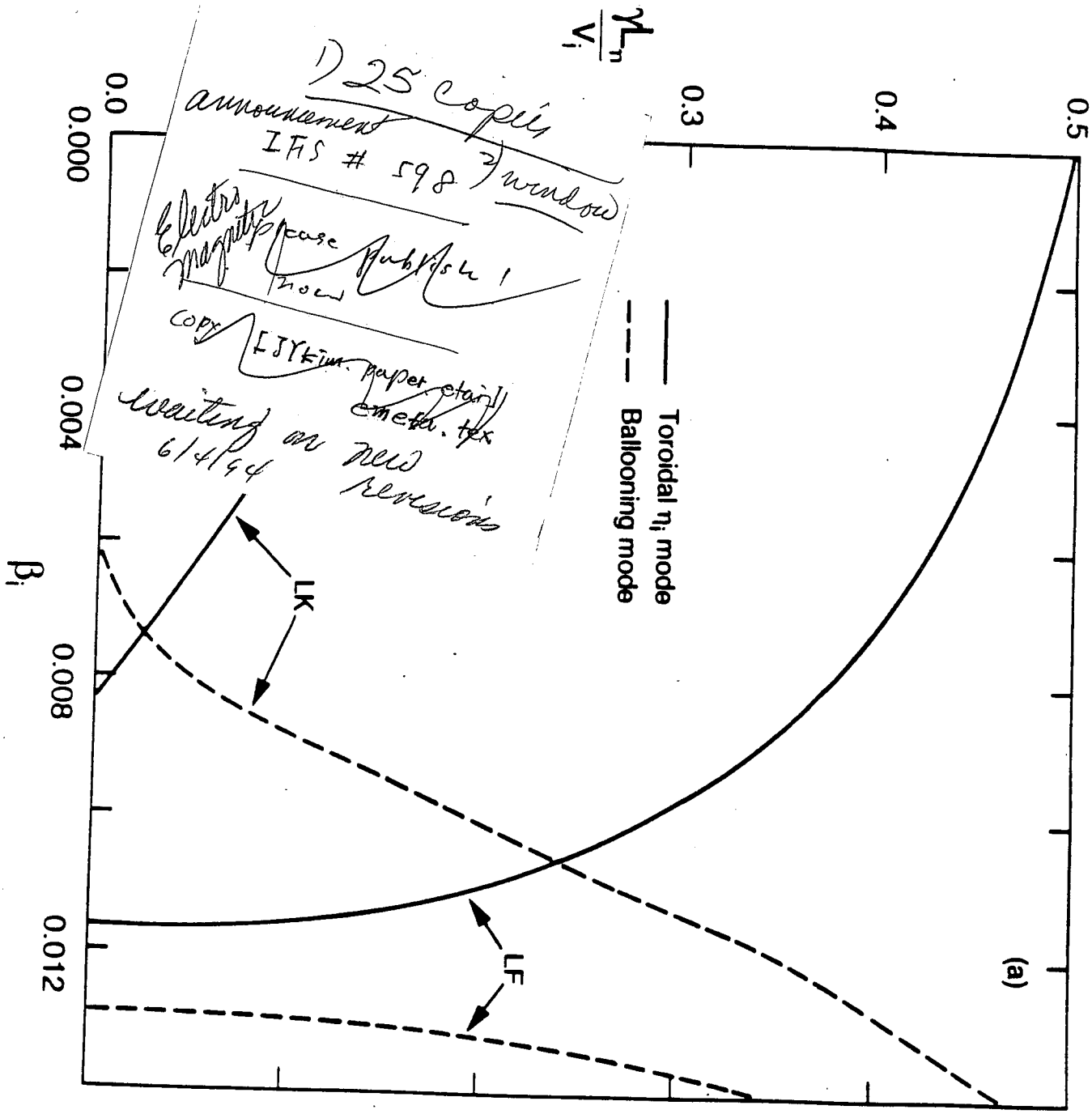

1) 25 copies announcement IFS # 598 2) window

Electro magnetic Please Publish now

copy EJY Kim. paper stain emetta.tex

waiting on new revisions 6/4/94

Fig. 1(a)

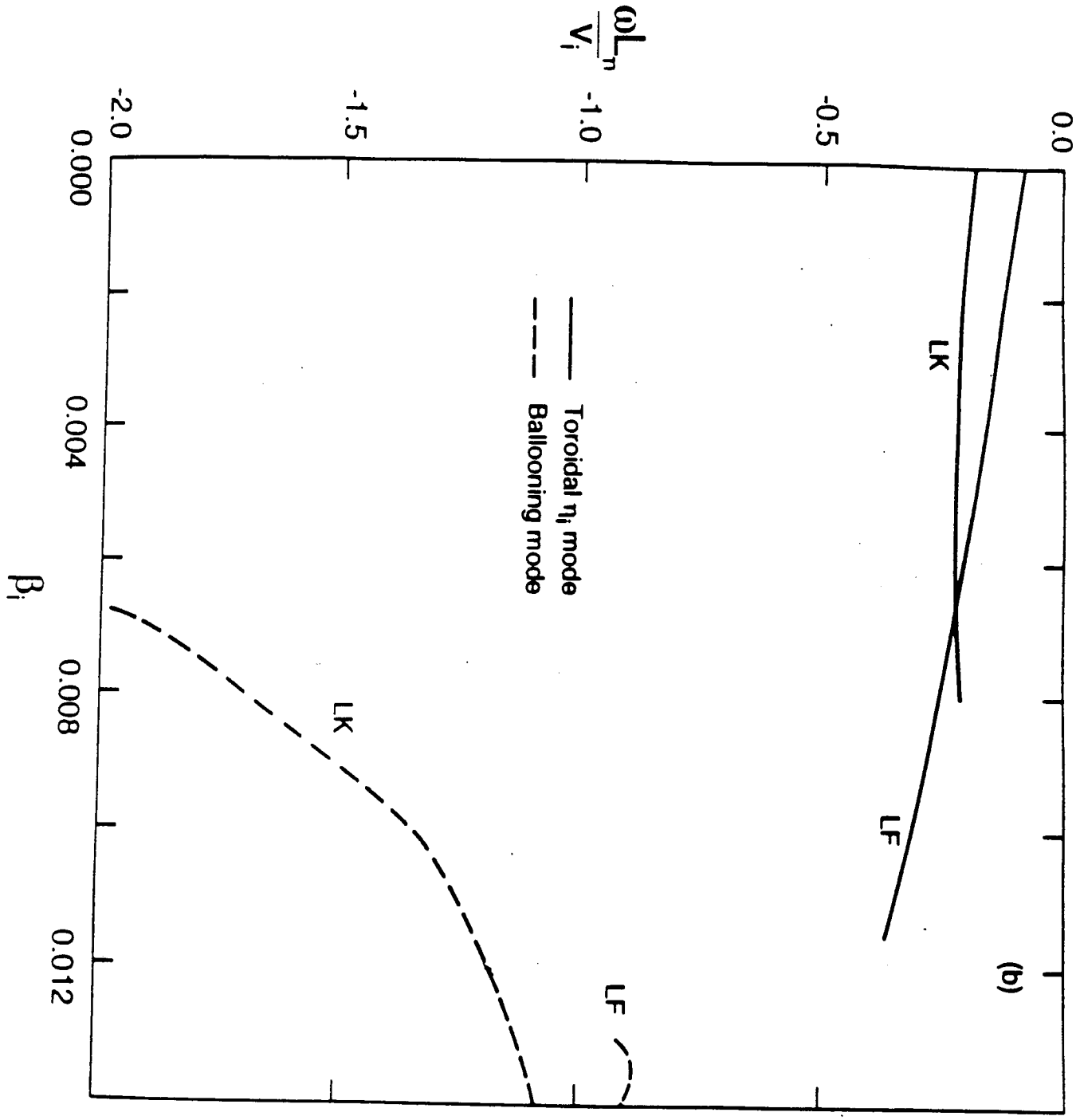
0.0
-0.5
-1.0
-1.5
-2.0
$\frac{\omega L_n}{V_i}$
0.000
0.004
0.008
0.012
β_i
LK
LF
(b)
Toroidal η_i mode
Ballooning mode
LK
LF

Fig. 1(b)

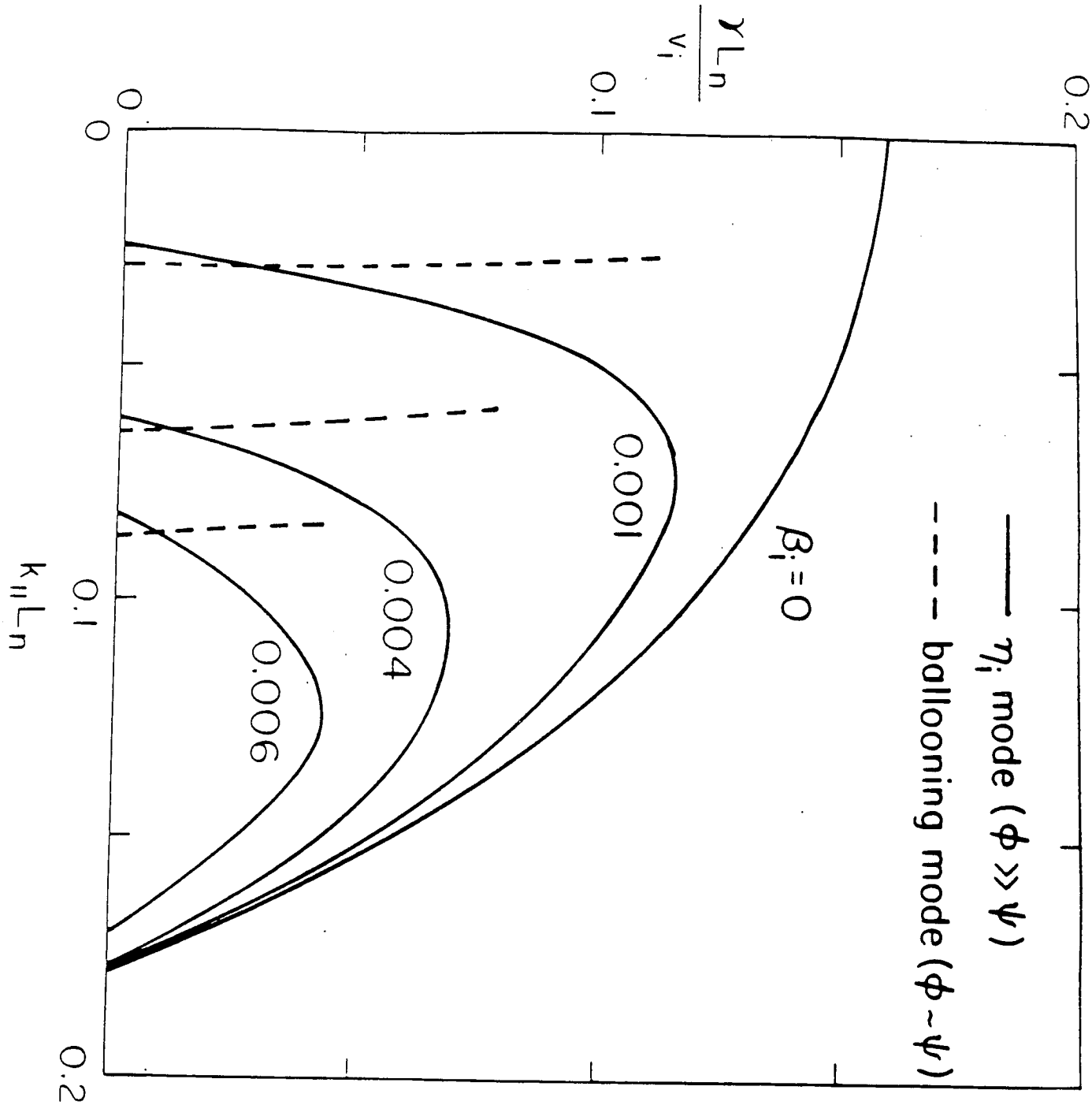
0.2
$\frac{\gamma L_n}{v_i}$
0.1
0
0
0.001
0.004
0.006
$\beta_i = 0$
η_i mode ($\phi \gg \psi$)
ballooning mode ($\phi \sim \psi$)
0.1
$k_{\parallel} L_n$
0.2

Fig. 2

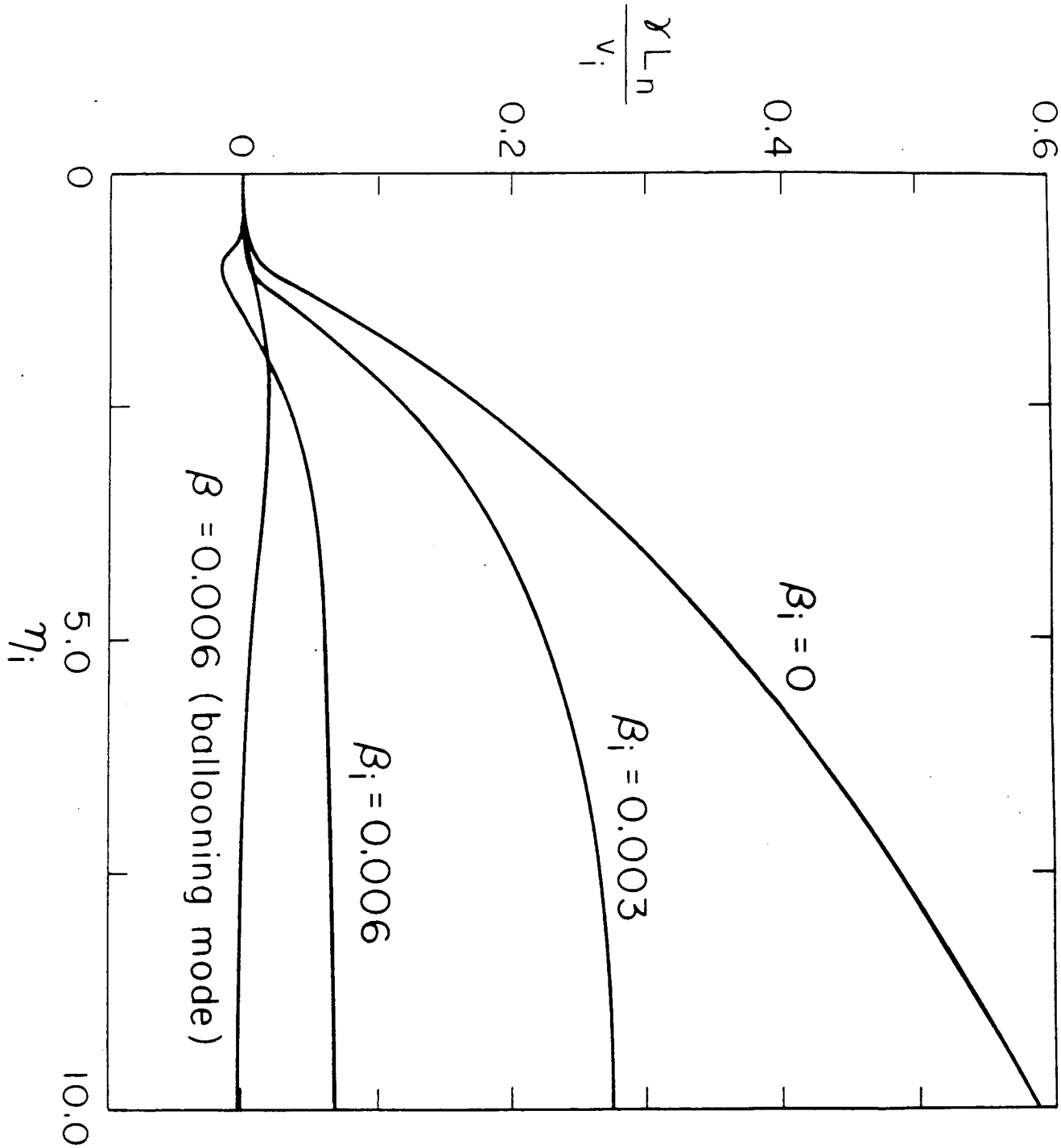
0.6
0.4
0.2
0
$\frac{\gamma L_n}{v_i}$
$\beta_i = 0$
$\beta_i = 0.003$
$\beta_i = 0.006$
$\beta = 0.006$ (ballooning mode)
0
5.0
10.0
η_i

Fig. 3

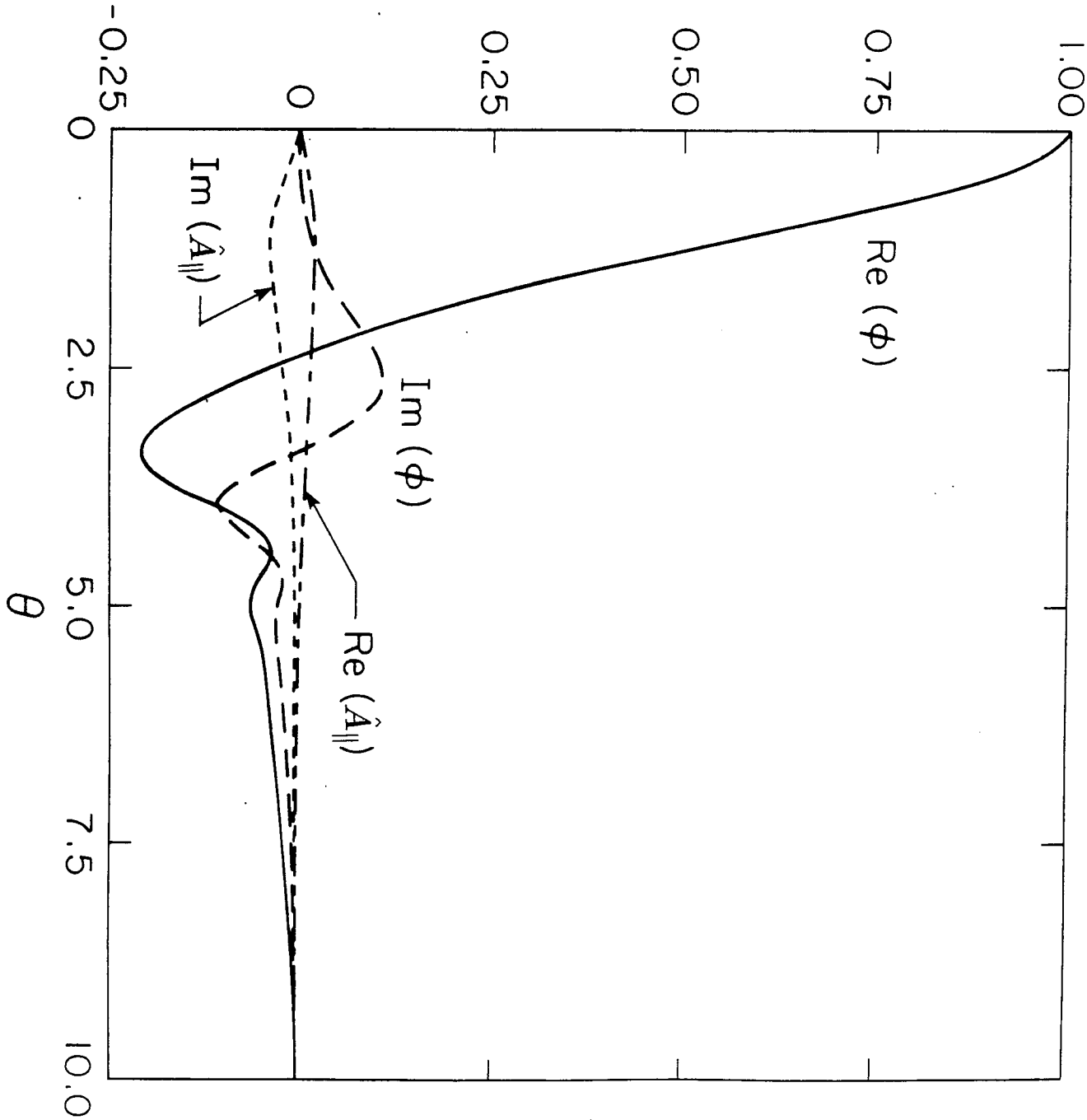
1.00
0.75
0.50
0.25
0
-0.25
Re (ϕ)
Im (ϕ)
Re ($\hat{A}_{\parallel}$)
Im ($\hat{A}_{\parallel}$)
0
2.5
5.0
7.5
10.0
θ

Fig. 4

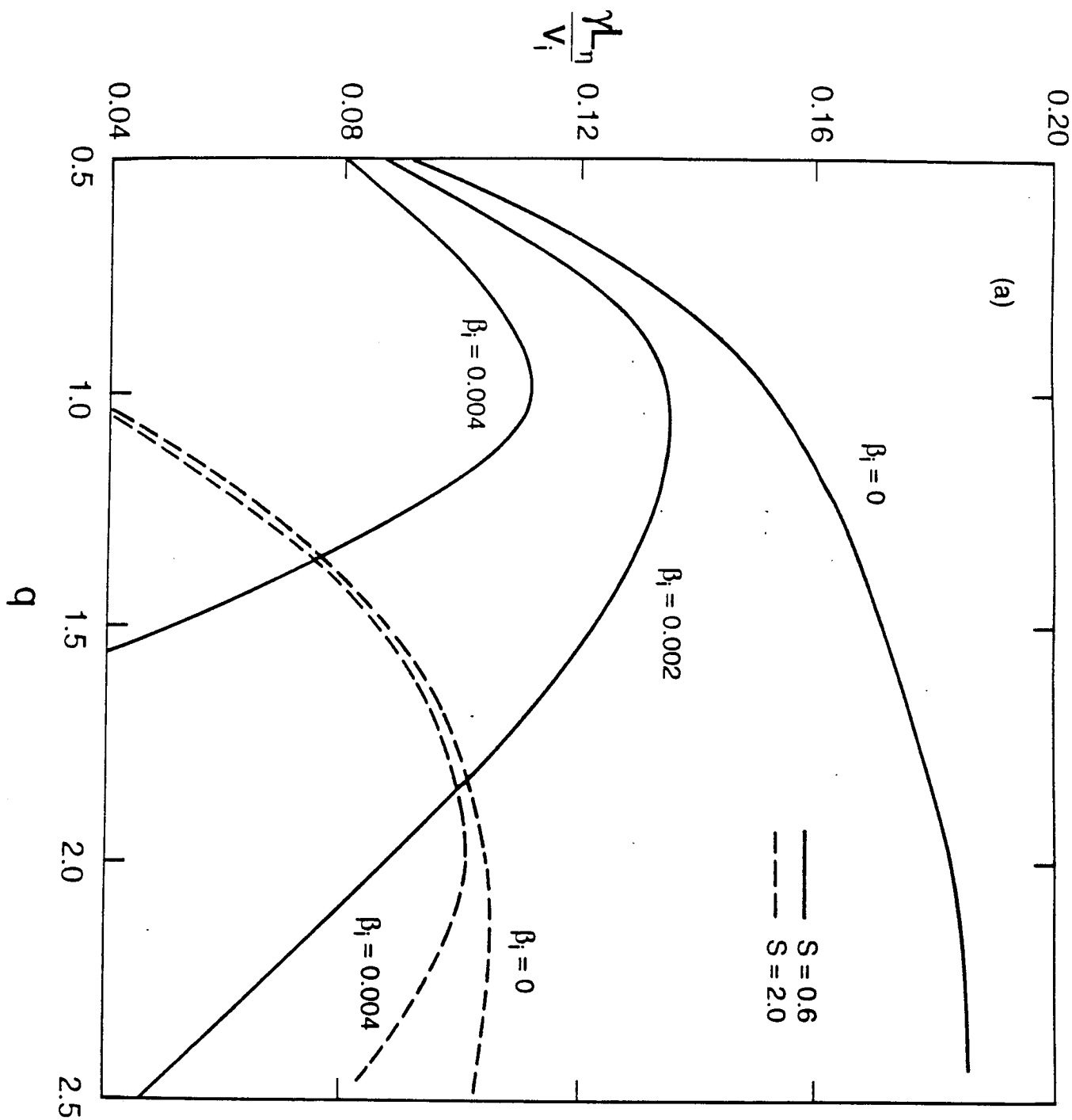
(a)
$\beta_i = 0$
$\beta_i = 0.002$
$\beta_i = 0.004$
$\beta_i = 0$
$\beta_i = 0.004$
S = 0.6
S = 2.0
$\frac{\gamma L_\eta}{v_i}$
q
0.20
0.16
0.12
0.08
0.04
0.5
1.0
1.5
2.0
2.5

Fig. 5(a)

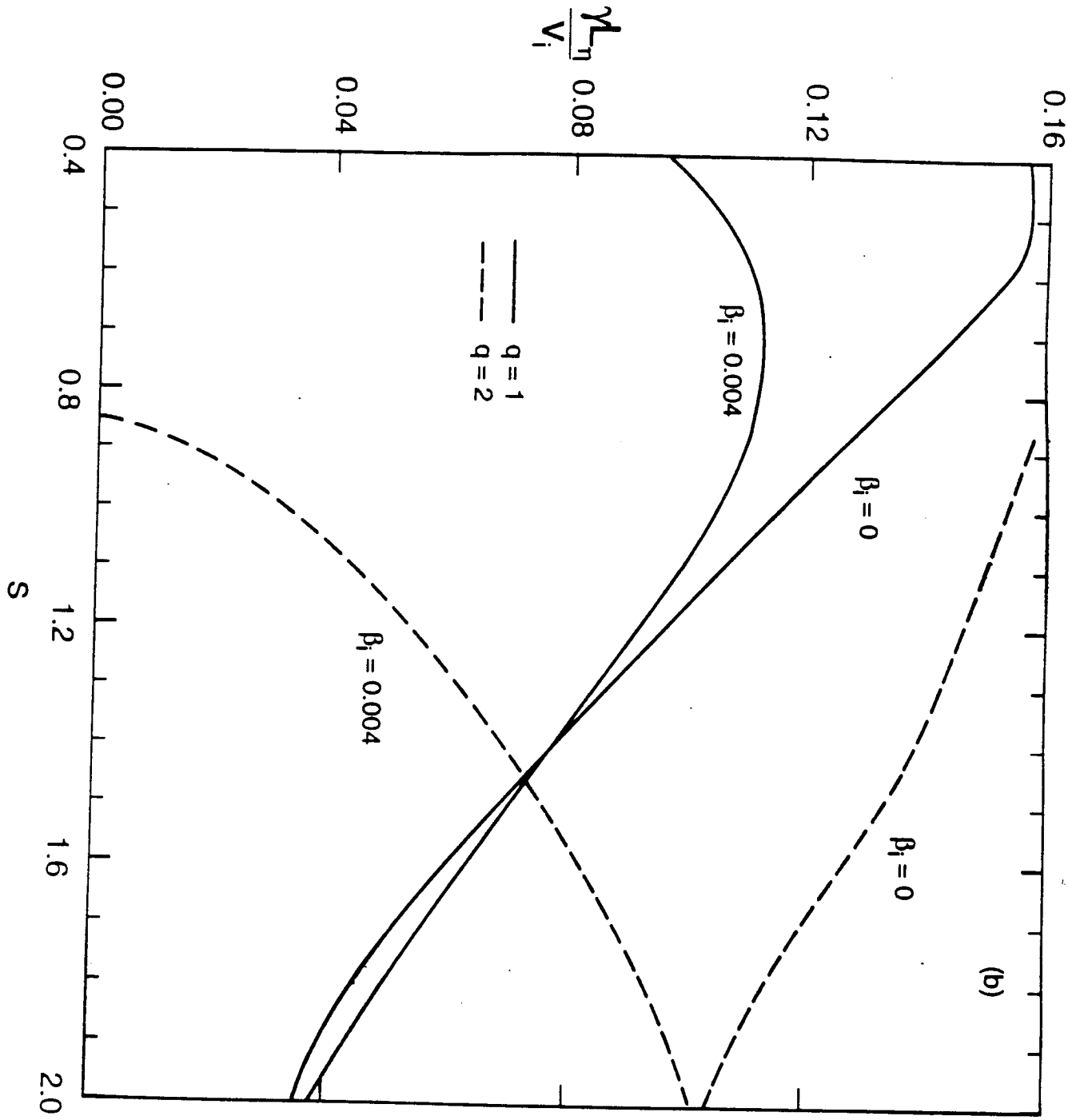
0.16
0.12
0.08
0.04
0.00
$\frac{\gamma L_\eta}{V_i}$
0.4
0.8
1.2
1.6
2.0
S
(b)
$\beta_i = 0$
$\beta_i = 0$
$\beta_i = 0.004$
$\beta_i = 0.004$
q = 1
q = 2

Fig. 5(b)